



CERN-EP/2016-199

2016/11/23

CMS-HIN-15-011

Decomposing transverse momentum balance contributions for quenched jets in PbPb collisions at $\sqrt{s_{\text{NN}}} = 2.76 \text{ TeV}$

The CMS Collaboration*

Abstract

Interactions between jets and the quark-gluon plasma produced in heavy ion collisions are studied via the angular distributions of summed charged-particle transverse momenta (p_T) with respect to both the leading and subleading jet axes in high- p_T dijet events. The contributions of charged particles in different momentum ranges to the overall event p_T balance are decomposed into short-range jet peaks and a long-range azimuthal asymmetry in charged-particle p_T . The results for PbPb collisions are compared to those in pp collisions using data collected in 2011 and 2013, at collision energy $\sqrt{s_{\text{NN}}} = 2.76 \text{ TeV}$ with integrated luminosities of $166 \mu\text{b}^{-1}$ and 5.3 pb^{-1} , respectively, by the CMS experiment at the LHC. Measurements are presented as functions of PbPb collision centrality, charged-particle p_T , relative azimuth, and radial distance from the jet axis for balanced and unbalanced dijets.

Published in the Journal of High Energy Physics as doi:10.1007/JHEP11(2016)055.

1 Introduction

High transverse momentum (p_T) jets originating from partons produced in the initial hard scatterings in ultra-relativistic heavy ion collisions have been used successfully to study the properties of the quark-gluon plasma (QGP) [1]. The observation of the jet quenching phenomenon, first at the BNL RHIC [2, 3] and then at the CERN LHC [4–7], began the era of detailed experimental studies trying to assess both the redistribution of energy from the parton as it interacts with the QGP, and the possible QGP response to the propagating parton. In these studies, a suppression of strongly interacting hard probes has been observed, including suppression of charged-particle yields associated with jets when compared with pp data at the same center-of-mass energy. The dependence of jet quenching on the collision centrality (i.e. the degree of the overlap of the two colliding nuclei, with fully-overlapping nuclei defined as “0% central”), has also been established, with stronger quenching effects reported for more central collisions. Detailed studies at CMS and ATLAS report that not only the suppression of jet yields, but also the relative differences between the momenta of the leading and subleading jets in dijet events increase in more central collisions, indicating that the jet quenching effect depends on the path length of the parton traversing the medium [4–6]. Corresponding measurements from the most peripheral (i.e. least central) PbPb data in these studies and from pPb collisions [8] are found to be similar to those in pp collisions, implying that the jet quenching phenomenon is caused by hot nuclear matter effects. Recently, CMS reported results showing the difference in the distribution of charged-particle p_T between the subleading and leading jet hemispheres in PbPb events with asymmetric dijets [9]. In these results, it is found that low- p_T particles extending to large angles away from the dijet axis in the subleading hemisphere must be considered in order to recover the momentum balance in these events. In addition to these momentum balance studies, precise measurements of the fragmentation pattern [10] and the distribution of charged-particle p_T as a function of radial distance from the jet axis [11], have also shown that the jet structure is modified by the medium. These modifications extend to large distances in relative pseudorapidity ($\Delta\eta$) and relative azimuth ($\Delta\phi$) with respect to the jet axis [12]. These studies have found softening of the jet fragmentation in PbPb collisions with respect to pp events, with the most significant excess of soft-hadron yields observed in more central PbPb events.

The analysis presented in this paper probes the details of the momentum distribution in dijet events, taking advantage of the high production rates for dijet events at the LHC, and the CMS detector’s ability to measure charged-particle tracks over an extended η and p_T range. Two-dimensional correlations between the reconstructed jets and charged-particle tracks (jet-track correlations) are constructed in $\Delta\eta$ and $\Delta\phi$. These correlations are used to decompose the overall event p_T distribution into three components: two 2D Gaussian-like peaks associated with the leading and subleading jets, and an azimuthal asymmetry in the distribution of momentum under the jet peaks. Results for each component are presented as a function of $\Delta\phi$, and the jet momentum density profile (“jet shape”) is also presented as a function of the radial distance from the jet axis in the $\Delta\eta$ - $\Delta\phi$ plane. Measurements are performed differentially in collision centrality, charged-particle transverse momentum (p_T^{trk}), and dijet asymmetry. These detailed differential studies provide input for theoretical models that attempt to describe the patterns of energy loss by a highly-energetic probe passing through the QGP.

The data used in this analysis are from PbPb collisions at a nucleon-nucleon center-of-mass energy of 2.76 TeV, corresponding to an integrated luminosity of $166 \mu\text{b}^{-1}$. For the reference measurement, pp data taken in 2013 at the same energy corresponding to an integrated luminosity of 5.3 pb^{-1} are used. These studies allow for a detailed characterization of the two-dimensional (in $\Delta\eta$ and $\Delta\phi$) p_T^{trk} distributions for charged-particle tracks with respect to the jet axes, provid-

ing information about the topology of the event from the jet perspective and details about the p_T^{trk} flow modification in dijet events.

In this paper, Section 2 gives general information about the CMS detector, and Section 3 outlines jet and track reconstruction procedures for PbPb and pp data. Section 4 describes the selection of events, while Section 5 details the procedure applied to analyze these events and evaluate systematic uncertainties. Section 6 presents results as a function of Δr (Section 6.1), $\Delta\phi$ (Section 6.2), and integrated transverse momentum balance over the whole event (Section 6.3). Finally, Section 7 summarizes and concludes the paper.

2 The CMS detector

The central feature of the CMS apparatus is a superconducting solenoid of 6 m internal diameter, providing a magnetic field of 3.8 T. Within the solenoid volume are a silicon pixel and strip tracker, a lead tungstate crystal electromagnetic calorimeter (ECAL), and a brass and scintillator hadron calorimeter (HCAL), each composed of a barrel and two endcap sections. Two hadronic forward (HF) steel and quartz-fiber calorimeters complement the barrel and endcap detectors, providing coverage up to $|\eta| < 5.2$. In this analysis, the collision centrality is determined using the total sum of transverse energy (E_T) from calorimeter towers in the HF region (covering $2.9 < |\eta| < 5.2$). The E_T distribution is used to divide the event sample into bins, each representing 0.5% of the total nucleus-nucleus hadronic interaction cross section. A detailed description of centrality determination can be found in Ref. [6].

Jet reconstruction for this analysis relies on calorimeter information from the ECAL and HCAL. For the central region ($|\eta| < 1.74$) from which jets are selected for this analysis, the HCAL cells have widths of 0.087 in both η and ϕ . In the η - ϕ plane, and for $|\eta| < 1.48$, the HCAL cells map on to 5×5 ECAL crystal arrays to form calorimeter towers projecting radially outwards from close to the nominal interaction point. Within each tower, the energy deposits in ECAL and HCAL cells are summed to define the calorimeter tower energies, subsequently used to provide the energies and directions of hadronic jets [13].

Accurate particle tracking is critical for measurements of charged-hadron yields. The CMS silicon tracker measures charged particles within the range $|\eta| < 2.5$. It consists of 1,440 silicon pixel and 15,148 silicon strip detector modules. For nonisolated particles of $1 < p_T < 10$ GeV and $|\eta| < 1.4$, the track resolutions are typically 1.5% in p_T and 25–90 (45–150) μm in the transverse (longitudinal) impact parameter [14]. Performance of the track reconstruction in pp and PbPb collisions will be discussed in Section 3.

A detailed description of the CMS detector, together with a definition of the coordinate system used and the relevant kinematic variables, can be found in [15].

3 Jet and track reconstruction

For both pp and PbPb collisions, jet reconstruction in CMS is performed with the anti- k_T algorithm, as implemented in the FastJet framework [16, 17], using a distance parameter $R = 0.3$. Jets are reconstructed offline (i.e. after raw data is recorded) based on energy deposits in the CMS calorimeters. Raw jet energies are obtained from the sum of the tower energies and raw jet momenta from the vectorial sum of the tower momenta, and are corrected to establish a relative uniform response of the calorimeter in η and a calibrated absolute response in p_T . For PbPb collisions, the CMS algorithm “HF/Voronoi” is used to estimate and subtract the heavy-ion underlying event based on information from HF energy measurements as well as Voronoi

decomposition of particle flow [9, 18]. For pp collisions, the contribution from the underlying event is negligible and no underlying event subtraction is employed.

Monte Carlo (MC) event generators have been used for evaluation of the jet and track reconstruction performance. Jet events are generated by the PYTHIA MC generator [19] (version 6.423, tune Z2 [20]). Simulated events are further propagated through the CMS detector using the GEANT4 package [21] to simulate the detector response. In order to account for the influence of the underlying PbPb event, the PYTHIA events are embedded into fully simulated PbPb events, generated by HYDJET [22] (version 1.8) that is tuned to reproduce the total particle multiplicities, charged-hadron spectra, and elliptic flow at all centralities. The embedding is done by mixing the simulated signal information from PYTHIA and HYDJET, hereafter referred to as PYTHIA+HYDJET. These events are then propagated through the same jet and track reconstruction and analysis procedures as pp and PbPb data.

The jet energy scale (JES) is established for pp using PYTHIA events and for PbPb using PYTHIA+HYDJET events in classes of event centrality. The accuracy of the reconstruction and correction procedure is tested as a function of jet p_T and η , by comparing a sample of reconstructed and corrected jets to the jets originally simulated in that sample. To account for the dependence of the JES on the fragmentation of jets, an additional correction is applied as a function of reconstructed jet p_T and as a function of the number of tracks with $p_T > 2\text{ GeV}$ within a radius $\Delta r < 0.3$ around the jet axis. This correction is derived separately for pp and PbPb data, as described in Ref. [9].

For studies of pp data and PYTHIA simulation, tracks are reconstructed using the same iterative method [14] as in the previous CMS analyses of pp collisions. For PbPb data and PYTHIA+HYDJET simulation, a dedicated heavy-ion iterative track reconstruction method [11, 23] is employed. Tracking efficiency for charged particles in pp collisions ranges from approximately 80% at $p_T \approx 0.5\text{ GeV}$ to 90% or better at $p_T \approx 10\text{ GeV}$ and higher. Track reconstruction is more difficult in the heavy-ion environment due to the high track multiplicity, and tracking efficiency for PbPb collisions ranges from approximately 30% at 0.5 GeV to about 70% at 10 GeV. Detailed studies of tracking efficiency and of tracking efficiency corrections (derived as a function of centrality, p_T^{trk} , η , ϕ , and local charged particle density) can be found in Ref. [9].

4 Event selection

The events for this analysis are selected using the CMS high-level trigger (HLT), with an inclusive single-jet trigger with a threshold of $p_T > 80\text{ GeV}$ [24]. This trigger is fully efficient in both PbPb and pp data for events containing offline reconstructed jets with $p_T > 120\text{ GeV}$. In order to suppress noncollision-related noise due to sources such as cosmic rays and beam backgrounds, the events used in this analysis are also required to satisfy offline selection criteria as documented in Refs. [6, 25]. These include restricting PbPb events to those containing a reconstructed vertex with at least two tracks and a z position within 15 cm of the detector center, and in which at least 3 GeV energy is deposited in at least three HF calorimeter towers on each side of the interaction point.

A dijet sample is selected using criteria matched to those of previous CMS analyses measuring dijet energy balance and correlated yields to high- p_T jets [5, 9, 12]. In this selection, events are first required to contain a leading calorimeter jet with $p_{T,1} > 120\text{ GeV}$ in the range of $|\eta_{\text{jet}}| < 2$, and a subleading jet of $p_{T,2} > 50\text{ GeV}$, also in $|\eta_{\text{jet}}| < 2$. Once the leading and subleading jets in the event have been identified, a tighter $|\eta_{\text{jet}}|$ selection is applied to ensure stable jet reconstruction performance and good tracker acceptance for tracks on all sides of each jet: only

events in which both leading and subleading jets fall within $|\eta_{\text{jet}}| < 1.6$ are included in the final selected data sample. The azimuthal angle between the leading and subleading jets is required to be at least $5\pi/6$. No explicit requirement is made either on the presence or absence of a third jet in the event. This jet sample is further divided based on the asymmetry between the leading and subleading jets, $A_J = (p_{T,1} - p_{T,2})/(p_{T,1} + p_{T,2})$. Two asymmetry classes are considered: the more balanced part (defined by $A_J < 0.22$) of the total dijet sample, and the more unbalanced part (defined by $A_J > 0.22$). The dividing value $A_J = 0.22$ is chosen for consistency with previous CMS analyses [5, 9]. In this analysis, 52% of PbPb events are balanced, while 67% of pp events are balanced. For the PbPb data, the centrality of the collisions is also considered and results are compared for central events (with centrality 0–30%) versus peripheral events (with centrality 50–100%).

5 Analysis procedure

Dijet events in this analysis are studied differentially in collision centrality, with the following bins: 0–30% (most central), 30–50% (not shown), and 50–100% (most peripheral). This analysis follows the procedure established in Refs. [12, 26]: two-dimensional $\Delta\eta$ – $\Delta\phi$ correlations with respect to the measured subleading and leading jet axes are constructed for charged-particle tracks in the event with $p_T^{\text{trk}} \geq 0.5 \text{ GeV}$ and $|\eta_{\text{track}}| < 2.4$, in several p_T^{trk} bins. These correlations are weighted by p_T^{trk} on a per-track basis, and normalized by the number of jets in the sample. This produces two-dimensional $\Delta\eta$ – $\Delta\phi$ average per-jet distributions of p_T^{trk} with respect to the leading and subleading jets. After the construction of the initial two-dimensional correlations described above, the remaining analysis procedure consists of the following steps, which will be discussed in detail below:

- A pair-acceptance correction, derived by the “mixed event” method [12, 26];
- The separation of correlations into jet-peak and long-range components;
- Corrections for jet reconstruction biases: a full simulation-based analysis is conducted to determine and subtract the correlated yield produced by jet selection bias.

5.1 Pair-acceptance correction

With jet acceptance of $|\eta_{\text{jet}}| < 1.6$, many tracks within $|\Delta\eta| < 2.5$ of a jet will fall outside of the track acceptance of $|\eta_{\text{track}}| < 2.4$, resulting in correlation geometry that falls with increasing $\Delta\eta$. To correct for this pair-acceptance effect, a mixed-event distribution is constructed by correlating jets from the jet-triggered event sample with tracks from a sample of minimum bias events, matched in vertex position (within 1 cm) and collision centrality (within 2.5%), following the technique used in Refs. [27–29]. In the following, N_{jets} denotes the number of dijet events selected as described in a given data sample. The per-jet associated yield, weighted per-track by p_T^{trk} is defined as:

$$\frac{1}{N_{\text{jets}}} \frac{d^2 \sum p_T}{d\Delta\eta d\Delta\phi} = \frac{ME(0,0)}{ME(\Delta\eta, \Delta\phi)} S(\Delta\eta, \Delta\phi). \quad (1)$$

The signal pair distribution, $S(\Delta\eta, \Delta\phi)$, represents the p_T^{trk} -weighted yield of jet-track pairs normalized by N_{jets} from the same event:

$$S(\Delta\eta, \Delta\phi) = \frac{1}{N_{\text{jets}}} \frac{d^2 \sum p_T^{\text{same}}}{d\Delta\eta d\Delta\phi}. \quad (2)$$

The mixed-event pair distribution,

$$ME(\Delta\eta, \Delta\phi) = \frac{1}{N_{\text{jets}}} \frac{d^2 N^{\text{mix}}}{d\Delta\eta d\Delta\phi}, \quad (3)$$

is constructed to account for pair-acceptance effects, with N^{mix} denoting the number of mixed-event jet-track pairs.

Signal and mixed event correlations are both corrected for tracking efficiencies on a per-track basis, using the efficiency parametrization defined as a function of centrality, p_T^{trk} , η , ϕ , and local charged-particle density, as in Ref. [9]. The ratio $ME(0,0)/ME(\Delta\eta, \Delta\phi)$ establishes the correction normalization, with $ME(0,0)$ representing the mixed-event associated yield for jet-track pairs going in approximately the same direction and thus having full pair acceptance.

5.2 Separation of correlations into jet-peak and long-range components

After the mixed-event correction, correlations to the leading and subleading jets show a Gaussian-like peak confined to the region $|\Delta\eta| < 1.5$, on top of a significant combinatorial and long-range-correlated background. To separate the long-range azimuthally-correlated and uncorrelated distributions under the peaks from jets, the “sideband” regions $1.5 < |\Delta\eta| < 2.5$ of both the leading and subleading jet acceptance-corrected correlations are projected into $\Delta\phi$. Previous studies have found no $\Delta\eta$ -dependence of the long-range underlying event distributions in this $|\Delta\eta|$ range [12, 30]. Figure 1 illustrates these long-range distributions in $\Delta\phi$ for pp, most peripheral PbPb, and most central PbPb data for representative bins at low (upper panels) and high (lower panels) p_T^{trk} of the tracks in unbalanced dijet events (with $A_J > 0.22$). For illustration, the range $|\Delta\phi| < \pi/2$ of the leading and subleading long-range $\Delta\phi$ distributions are shown as a combined 2π distribution, with the subleading jet distribution shifted by π to show the full underlying event correlation with respect to the leading jet direction. The visible asymmetry in this long-range distribution in pp data is attributed to the presence of additional jets and other contributions that must, by momentum conservation, be present on the subleading side of the unbalanced dijet system.

To isolate the Gaussian-like leading and subleading jet peaks, this long-range distribution is propagated over the full range $|\Delta\eta| < 2.5$ and subtracted in 2D from the mixed-event-corrected signal correlation. In addition, the leading side of the long-range distribution is subtracted from the subleading side (in the illustration shown, the distribution for $|\Delta\phi| < \pi/2$ is subtracted from the distribution for $\pi/2 < \Delta\phi < 3\pi/2$) to obtain a measurement of subleading-to-leading asymmetry in the long-range correlated background. With this, the three contributions to the dijet hemisphere momentum balance have been identified: leading jet peak, subleading jet peak, and subleading-to-leading two-dimensional underlying event asymmetry.

5.3 Corrections and systematic uncertainties

Simulation-based corrections are applied to correlations to account for two biases in jet reconstruction: a bias toward selecting jets that are found on upward fluctuations in the background (relevant for PbPb only), and a bias toward selecting jets with harder fragmentation (affecting PbPb and pp similarly). For the former, to estimate and subtract the contribution to the excess yield due to background fluctuation bias in jet reconstruction, a similar procedure to that outlined in previous CMS studies [10] is followed. Simulations are performed in PYTHIA+HYDJET samples with reconstructed jets, and correlations are constructed excluding particles generated with the embedded PYTHIA hard-scattering process. A Gaussian fit to the excess is subtracted as a correction from the data results, and half its magnitude is assigned as the associated systematic uncertainty.

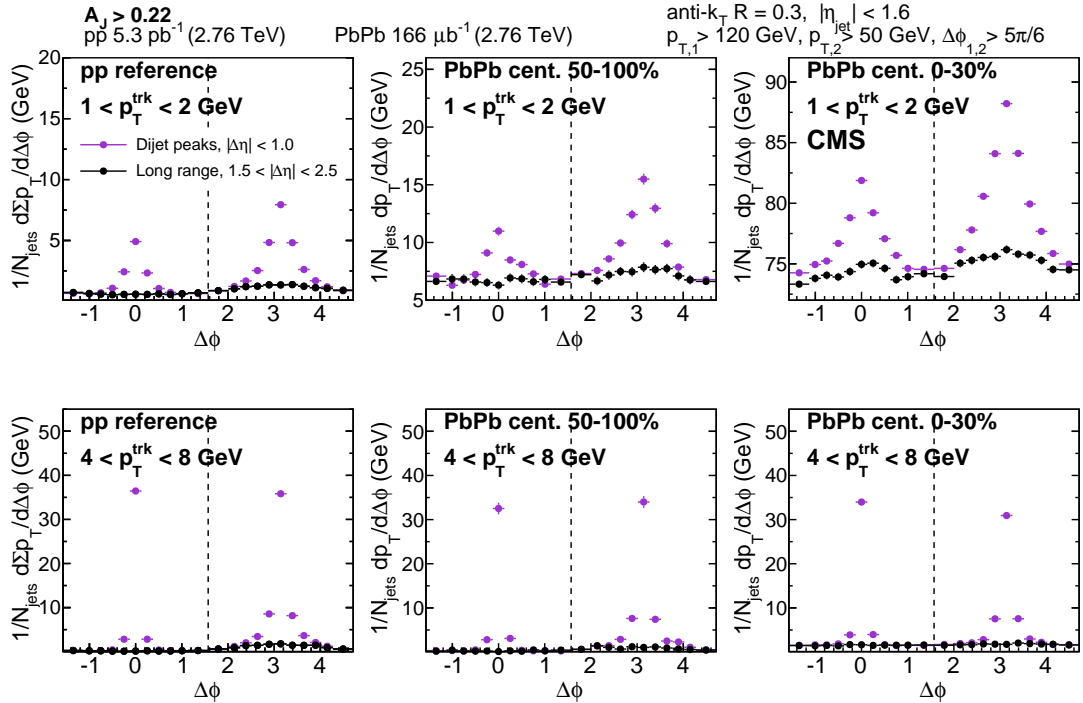


Figure 1: Jet-track correlation distributions for unbalanced dijet events ($A_J > 0.22$), projected over $|\Delta\eta| < 1$, and overlaid with a long-range distribution projected over $1.5 < |\Delta\eta| < 2.5$. The region $|\Delta\phi| < \pi/2$ is taken from the leading jet correlation, while the region $\pi/2 < \Delta\phi < 3\pi/2$ is taken from the subleading jet correlation. The top row shows the low p_T^{trk} bin $1 < p_T^{\text{trk}} < 2 \text{ GeV}$, while the bottom row shows the high p_T^{trk} bin $4 < p_T^{\text{trk}} < 8 \text{ GeV}$. Statistical uncertainties are shown with vertical bars.

The second bias is toward the selection of jets with fewer associated tracks in both pp and PbPb data for all p_T^{trk} selections studied, due to the fact that jets with harder fragmentation are more likely to be successfully reconstructed than jets with softer fragmentation. Following the method used in Refs. [9, 12], corrections are derived for this jet fragmentation function (JFF) bias and for the related possible effect of "jet swapping" between leading, subleading, and additional jets by comparing correlated per-trigger particle yields for all reconstructed jets versus all generated jets. This correction is derived for each jet selection in a PYTHIA-only simulation, and also in PYTHIA+HYDJET events, excluding HYDJET tracks from the correction determination. The variation between the JFF and jet swapping correction derived from PYTHIA embedded into HYDJET simulation at different centralities is assigned as a systematic uncertainty in this correction. This uncertainty is less than 2% for all p_T^{trk} selections, and converges to zero at high p_T^{trk} .

Jet reconstruction-related sources of systematic uncertainty in this analysis include the two reconstruction biases as discussed above, as well as a residual JES uncertainty that accounts for possible differences of calorimeter response in data and simulation. In simulation, for example, there is a difference in the JES between quark and gluon jets (about 2% at 120 GeV [9]), meaning that medium-induced changes in jet flavor could result in either over-correction or under-correction of jet energy, and a resulting bias in jet selection. To evaluate this residual JES uncertainty, we vary the leading jet selection threshold by 3% to account for possible differences in data versus simulated calorimeter response. The resulting maximum variations in total correlated particle yield are found to be within 3% in all cases, and we conservatively assign 3% to account for this systematic uncertainty source.

The tracking efficiency correction uncertainty is estimated from the ratio of corrected reconstructed yields and generated yields in PYTHIA and PYTHIA+HYDJET simulated events, by using generator-level charged particles as a reference. This uncertainty is found to be $\sim 2\text{--}4\%$ for PbPb and pp collisions, with the greater value corresponding to a higher multiplicity and lower momentum range of selected tracks. To account for possible track reconstruction differences in data and simulation, a residual uncertainty in track reconstruction efficiency and misidentification rate corrections is estimated to be 5% [9].

The uncertainty arising from pair acceptance effects is estimated by considering the sideband asymmetry after dividing by the mixed-event correlation. Each sideband region of the final background-subtracted $\Delta\eta$ distribution ($-2.5 < \Delta\eta < -1.5$ and $1.5 < \Delta\eta < 2.5$) is separately fit with a constant. The greater of these two deviations from zero is assigned as systematic uncertainty, and is found to be within 5–9% for the lowest p_T^{trk} bin. The uncertainty resulting from the event decomposition is determined by evaluating point-to-point variations in the side-band projections used to estimate long-range correlation contributions. The event decomposition uncertainty is found to be within 2–5% for 0–30% central PbPb data in the the lowest p_T^{trk} bin where the background is most significant compared to the signal level, and decreases for less central collisions and for higher p_T^{trk} tracks ($p_T^{\text{trk}} > 2\text{ GeV}$).

The systematic uncertainties from the sources discussed above are added in quadrature for the final result. Table 1 lists the upper limits on the estimated contributions from the individual sources described above.

Table 1: This table summarizes the systematic uncertainties in the measurement of the jet-track correlations in PbPb and pp collisions. Upper and lower limits are shown as a function of collision centrality. Upper values correspond to the uncertainties at lowest p_T^{trk} .

Source	0–30%	30–50%	50–100%	pp
Balanced jet selection ($A_J < 0.22$):				
Background fluctuations	1–8%	1–3%	0–1%	—
JFF bias and jet swapping	0–2%	0–2%	0–2%	0–2%
Residual JES	3%	3%	3%	3%
Tracking efficiency	4%	4%	4%	3 %
Residual track efficiency corr.	5%	5%	5%	5%
Pair acceptance corrections	5–9%	4–8%	2–6%	2–3%
Event decomposition	2–5%	2–5%	2–5%	1–2%
Total	9–15%	8–13%	8–10%	7–8%
Unbalanced jet selection ($A_J > 0.22$):				
Background fluctuations	1–10%	1–5%	0–2%	—
JFF bias and jet swapping	0–2%	0–2%	0–2%	0–2%
Residual JES	3%	3%	3%	3%
Tracking efficiency	4%	4%	4%	3 %
Residual track efficiency corr.	5%	5%	5%	5%
Pair acceptance corrections	5–9%	4–8%	2–6%	2–3%
Event decomposition	2–5%	2–5%	2–5%	1–2%
Total	9–16%	8–13%	8–10%	7–8%

6 Results

In this analysis, two-dimensional $\Delta\eta$ - $\Delta\phi$ momentum distributions with respect to high- p_T leading and subleading jets are studied differentially in centrality and p_T^{trk} . First, the jet momentum density profile is measured as a function of $\Delta r = \sqrt{(\Delta\eta)^2 + (\Delta\phi)^2}$ for all dijet events, comparing PbPb to pp jet shapes up to $\Delta r = 1$. Next, the sample is divided into balanced ($A_J < 0.22$) and unbalanced ($A_J > 0.22$) dijet events, and the overall subleading-to-leading hemisphere momentum balance is evaluated by subtracting the distribution of p_T^{trk} about the leading jet from the distribution of p_T^{trk} about the subleading jet. This overall hemisphere momentum balance is then further decomposed into contributions from the leading and subleading jet peaks and from the underlying event-wide long-range asymmetry. The jet peak shapes are quite similar in $\Delta\eta$ and $\Delta\phi$, as reported in Ref. [12], but the long-range “ridge-like” distribution is independent of $\Delta\eta$ within the fiducial acceptance and uncertainties, while showing a clear $\Delta\phi$ dependence, as is visible in Fig. 1. To avoid convolving these two different trends, we present the results that follow as a function of $\Delta\phi$, including the overall subleading-to-leading hemisphere momentum balance and respective contributions from the leading and subleading peaks and underlying long-range asymmetry as a function of $\Delta\phi$. Finally, we summarize our findings by presenting the total momentum in each p_T^{trk} bin, integrated over each hemisphere.

6.1 Measurement of radial jet momentum density profile

After subtraction of the long-range background, p_T^{trk} correlations in $\Delta\eta$ and $\Delta\phi$ may be used to obtain measurements of jet shape as a function of Δr by direct integration. Jet shape $\rho(\Delta r)$ is defined as:

$$\rho(\Delta r) = \frac{1}{\delta r} \frac{1}{N_{\text{jets}}} \sum_{\text{jets}} \frac{\sum_{\text{tracks} \in (r_a, r_b)} p_T^{\text{trk}}}{p_T^{\text{jets}}}. \quad (4)$$

The jet shape $\rho(\Delta r)$ is extracted by integrating 2D jet-peak momentum distributions in annuli with radial width $\delta r = 0.05$, where each has an inner radius of $r_a = r - \delta r/2$ and outer radius of $r_b = r + \delta r/2$. A previous CMS study measured the jet shape $\rho(\Delta r)$ within the jet cone radius $\Delta r = 0.3$ [11]; for comparison with this previous result, distributions are normalized to integrate to unity within the radius $\Delta r < 0.3$. In Fig. 2, the leading jet shape measured with this correlation technique is compared to the published CMS measurement [11]. The new jet shape measurement is performed differentially in p_T^{trk} , in bins ranging from $0.5 < p_T^{\text{trk}} < 1 \text{ GeV}$ to $p_T^{\text{trk}} > 8 \text{ GeV}$. With the advantages provided by the correlation technique, the radial jet momentum density profile measurements are also extended in this analysis to $\Delta r = 1$. The $\Delta r = 1$ limit is driven by the pp data, which has no correlated yields within our sample at larger Δr . The leading jet shape is found to be very similar to that in the previous measurement for an inclusive jet selection of all jets with $p_T > 100 \text{ GeV}$, despite small differences in the jet selection.

A new measurement of subleading jet shape is presented in Fig. 3. Significant jet shape modifications are evident in central PbPb events for both leading and subleading jets with respect to the pp reference measurement, while in peripheral PbPb events the jet shapes are similar to the pp reference. Broadening of the jet structure is an expected consequence of jet quenching in theoretical models [31]. Here it is important to note that the broadening in central PbPb collisions is relative to the jets of the same type (leading or subleading) in pp collisions. The subleading jets are of lower p_T by selection in both PbPb and pp, and significantly broader than leading jets in pp data. Thus, although subleading jets in central PbPb collisions are softer and broader than leading jets in these collisions, the relative jet shape modification (expressed via a

ratio to pp data) is greater for leading jets since these are compared to the narrower pp leading jets.

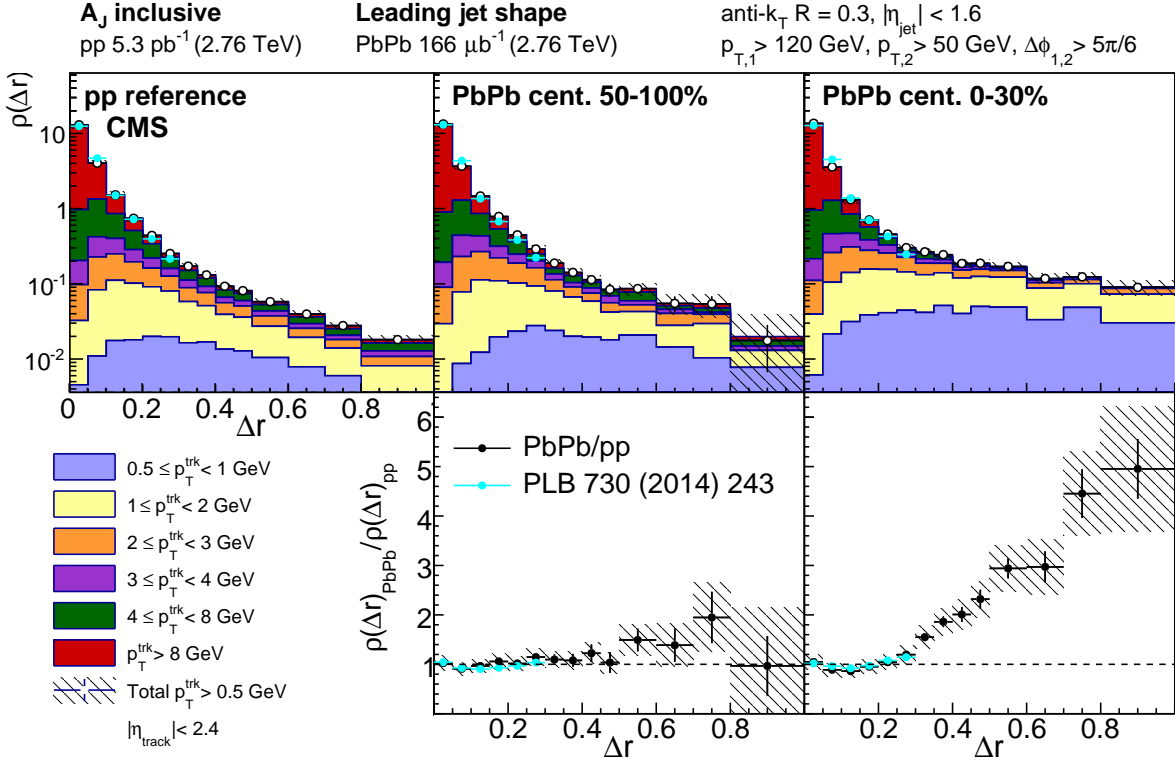


Figure 2: Top row: leading jet shape $\rho(\Delta r)$ for the pp reference, and peripheral and central PbPb data, shown for all tracks with $p_T > 0.5 \text{ GeV}$ and decomposed by p_T^{trk} (with p_T^{trk} ranges denoted by different color shading). Shapes are normalized to unity over the region $\Delta r < 0.3$ for comparison with the published reference shown (Ref. [11]). Bottom row: leading jet shape ratio $\rho(\Delta r)_\text{PbPb} / \rho(\Delta r)_\text{pp}$, again with the published reference. Statistical uncertainties are shown with vertical bars, and systematic uncertainties are shown with shaded boxes.

6.2 Azimuthal distribution of charged-particle transverse momentum

To investigate in detail how the modification of the jet peaks contributes to the overall redistribution of p_T^{trk} flow reported in [9], we measure the transverse momentum balance in the event via $\Delta\eta$ - $\Delta\phi$ p_T^{trk} correlations to subleading and leading jets. First, we present the hemisphere-wide balancing distribution of p_T^{trk} around the subleading versus the leading jets in Figs. 4 and 5, for balanced and unbalanced dijet events, respectively. These figures show the per-event azimuthal distribution of p_T^{trk} about the leading or subleading jet axis, denoted $P = 1/N_{\text{evt}} d\Sigma p_T / d\Delta\phi$, with the subleading-to-leading hemisphere difference of this distribution denoted ΔP . For display, all distributions are symmetrized in $\Delta\phi$. For both balanced and unbalanced dijet events, a broad excess of soft particles is evident in the subleading versus leading hemisphere in central PbPb collisions relative to the pp reference data. This reflects the greater quenching of the subleading jet. In the unbalanced selection, as required by the momentum conservation, the signal is enhanced in both pp and PbPb data: in pp data a large excess of particles with $p_T^{\text{trk}} > 3 \text{ GeV}$ is present on the subleading side. This excess compensates for the smaller contribution of the highest p_T particles in the jet itself. In peripheral PbPb data the distribution is quite similar to the pp reference, while in central PbPb data this balancing distribution consists mostly of soft particles with $p_T^{\text{trk}} < 3 \text{ GeV}$, consistent with the findings of

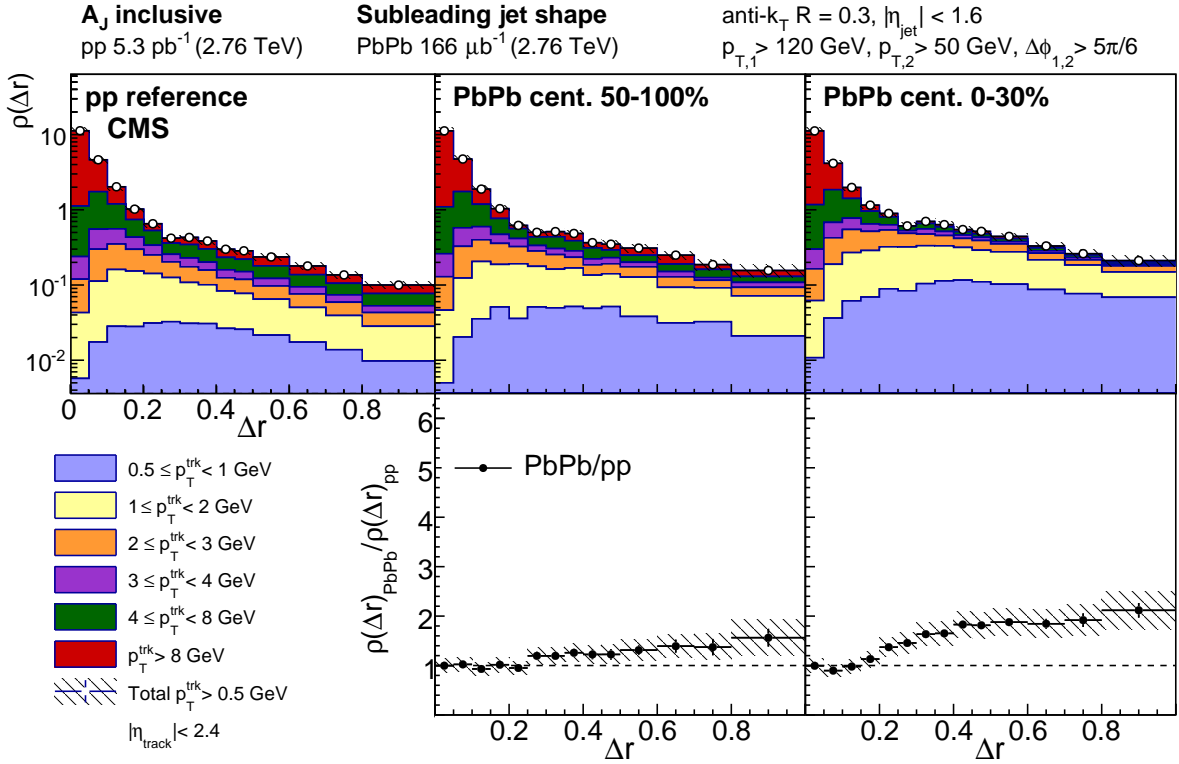


Figure 3: Top row: subleading jet shape $\rho(\Delta r)$ for pp reference and peripheral and central PbPb data, shown for all tracks with $p_T > 0.5 \text{ GeV}$ and decomposed by p_T^{trk} (with p_T^{trk} ranges denoted by different color shading), normalized to unity over the region $\Delta r < 0.3$. Bottom row: subleading jet shape ratio $\rho(\Delta r)_{\text{PbPb}} / \rho(\Delta r)_{\text{pp}}$. Statistical uncertainties are shown with vertical bars, and systematic uncertainties are shown with shaded boxes.

the previous CMS study [9]. To demonstrate these medium modifications more clearly, the difference in yield between PbPb and pp collisions is shown in the bottom panels of Figs. 4 and 5. For presentation, tracks with $p_T^{\text{trk}} > 8 \text{ GeV}$ are not included in these figures, so that it is possible to zoom in on the low- p_T^{trk} structures and modifications.

To elucidate the redistribution of p_T^{trk} within the QGP, the distributions are separated into three components as stated above: the two Gaussian-like peaks about the leading and subleading jet axes, and a third component accounting for overall subleading-to-leading hemisphere asymmetry of the long-range side-band distributions (measured in the region $1.5 < |\Delta\eta| < 2.5$). In Figs. 6 and 7, the jet peak components are shown for balanced and unbalanced jets, respectively, presenting subleading results as positive and leading results as negative (in line with the hemisphere difference measurements in Figs. 4 and 5). Jet peak distributions after decomposition are projected over the full range $|\Delta\eta| < 2.5$, again for consistency with the hemisphere difference measurements. The top row of each panel first shows the overall distribution of momentum carried by particles with $p_T^{\text{trk}} < 8 \text{ GeV}$ associated with the jet peak. The middle two panels then assess modifications to the subleading and leading jets for each p_T^{trk} bin. Here, again, there is evidence of quenching of both the subleading and leading jets in central PbPb collisions relative to the pp reference data. There is an excess of low- p_T particles correlated with the leading and subleading jet axes in both the balanced and unbalanced dijet selections, in agreement with results presented in the CMS study [12]. In unbalanced dijet events, this enhancement of soft particles turns into a depletion at higher p_T^{trk} , and is greater on the subleading than the leading side. The pp subleading jet peak is broader than the pp leading jet

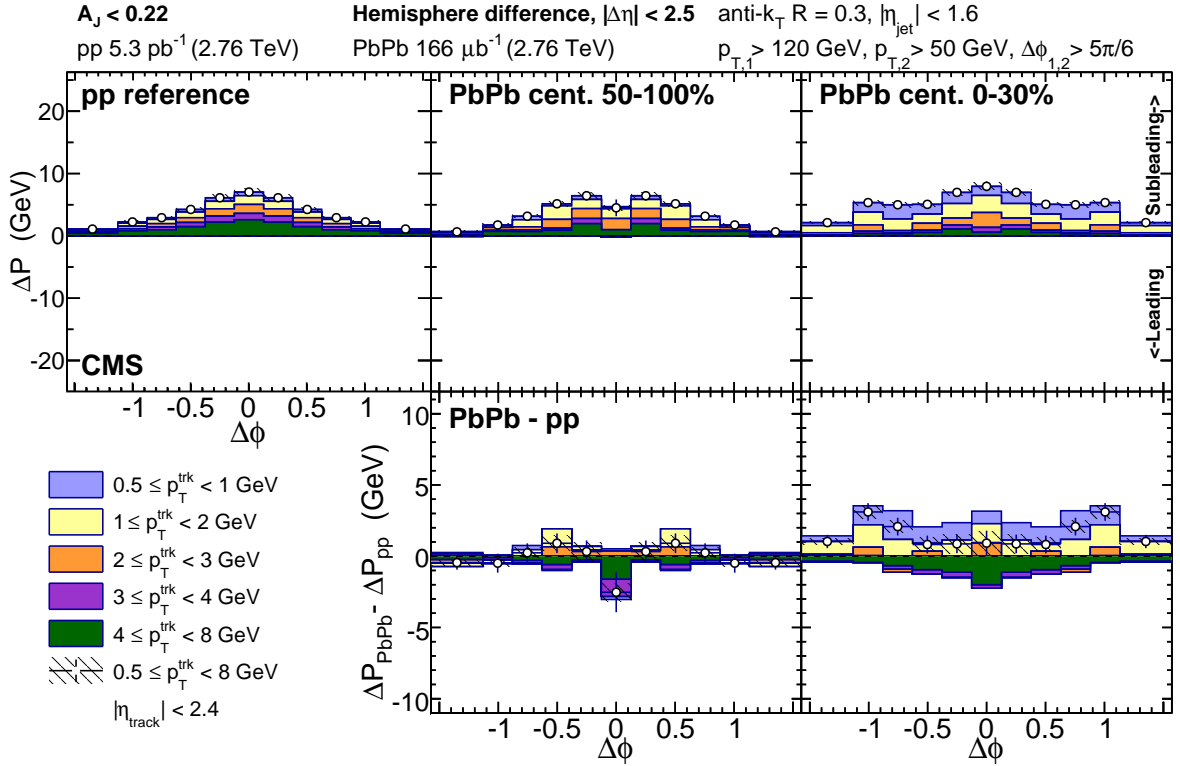


Figure 4: Top row: difference of the total p_T^{trk} distributions between subleading and leading jet hemispheres, projected on $\Delta\phi$, for balanced dijet events with $A_J < 0.22$ shown differentially by p_T^{trk} for pp reference, peripheral PbPb, and central PbPb data. Bottom row: PbPb-pp difference in these $\Delta\phi$ momentum distributions. Statistical uncertainties are shown with vertical bars, and systematic uncertainties are shown with shaded boxes.

peak and, while both subleading and leading jet peaks are broader in central PbPb than pp data, the PbPb-pp excess is wider on the leading than on the subleading side. To assess the jet peak contributions to the overall hemisphere momentum balance, the double-differential (PbPb-pp, subleading-leading) result is presented in the bottom panel. Here it is evident that the low- p_T^{trk} excess in central PbPb collisions is greater on the subleading than the leading side of the dijet system, but the larger subleading-to-leading excess only accounts for a portion of the total momentum redistribution in unbalanced dijet events. It is also clear that the high- p_T^{trk} large-angle depletion observed in the overall hemisphere momentum balance distribution is not produced by the Gaussian-like jet peaks.

To uncover the missing part of the total transverse momentum balance, these jet-related studies are complemented by an analysis of the long-range subleading-to-leading hemisphere asymmetry, presented in Figs. 8 and 9 for balanced and unbalanced jets, respectively. The long-range correlated background in balanced dijet events is approximately symmetric in pp and peripheral PbPb data, while in central PbPb data there is a small excess of low- p_T particles. In unbalanced dijet events, however, there is already significant asymmetry in the pp reference data, with a large correlated excess of particles in all p_T^{trk} classes less than 8 GeV on the subleading relative to the leading side of the underlying event. This asymmetry reflects the presence of other hard-scattering products in the subleading hemisphere of dijet events (e.g. additional jets), as required by the momentum conservation for asymmetric dijet events in pp collisions. In the presence of the strongly interacting medium, however, this underlying event asymmetry in asymmetric dijet events changes notably. In peripheral PbPb collisions, an onset of some

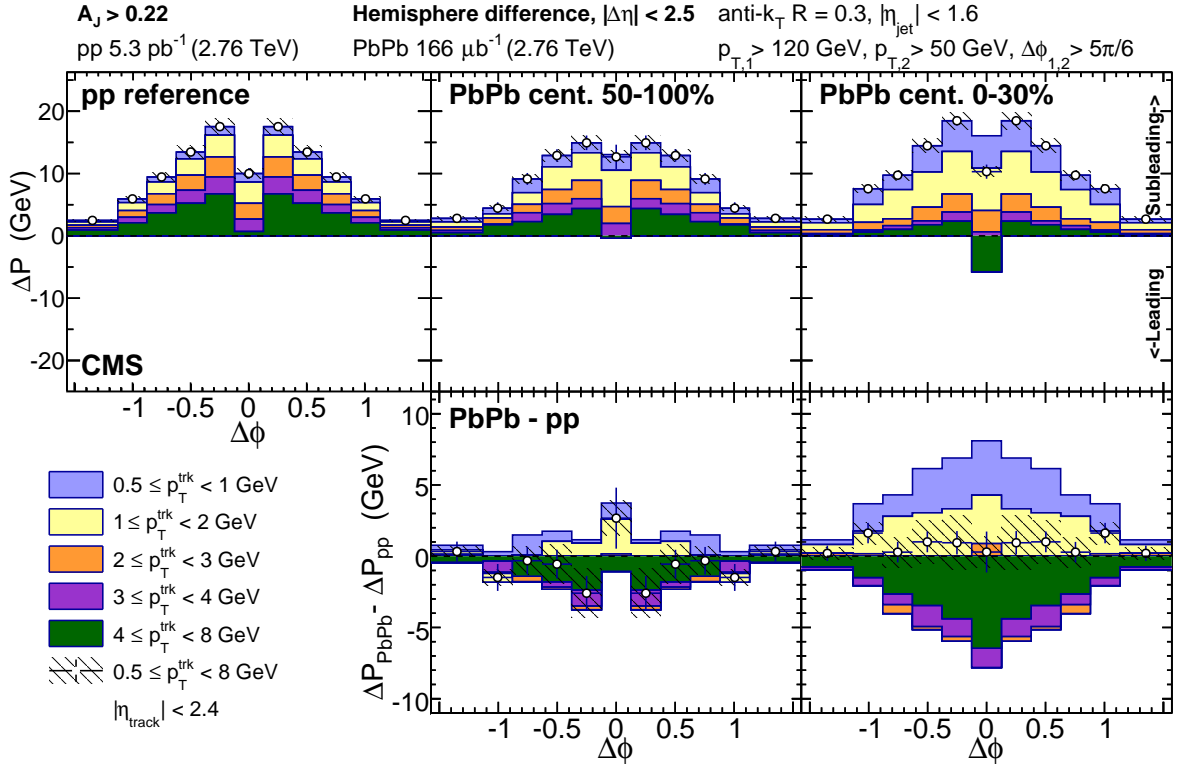


Figure 5: Top row: difference of the total p_T^{trk} distributions between subleading and leading jet hemispheres, projected on $\Delta\phi$, for unbalanced dijet events with $A_J > 0.22$, shown differentially by p_T^{trk} for the pp reference data, peripheral PbPb, and central PbPb data. Bottom row: PbPb–pp difference in these $\Delta\phi$ momentum distributions. Statistical uncertainties are shown with vertical bars, and systematic uncertainties are shown with shaded boxes.

depletion of momentum carried by high- p_T particles can be seen, and in central PbPb data, subleading-to-leading underlying event excesses with $p_T^{\text{trk}} > 2 \text{ GeV}$ nearly vanish. The significance of the contribution of this long-range asymmetry to the total hemisphere imbalance is further assessed by the double difference (PbPb–pp, subleading–leading), which is shown on the bottom panel. The absence of a high- p_T^{trk} component in the long-range part of the correlation suggests that events containing additional jets constitute a smaller fraction of unbalanced dijet events in PbPb than pp data. A likely explanation for this effect is that while momentum conservation requires the presence of additional jets in unbalanced pp dijet events, in PbPb data the sample of unbalanced dijet events also includes events in which the dijet asymmetry is due to the greater quenching of the subleading jet.

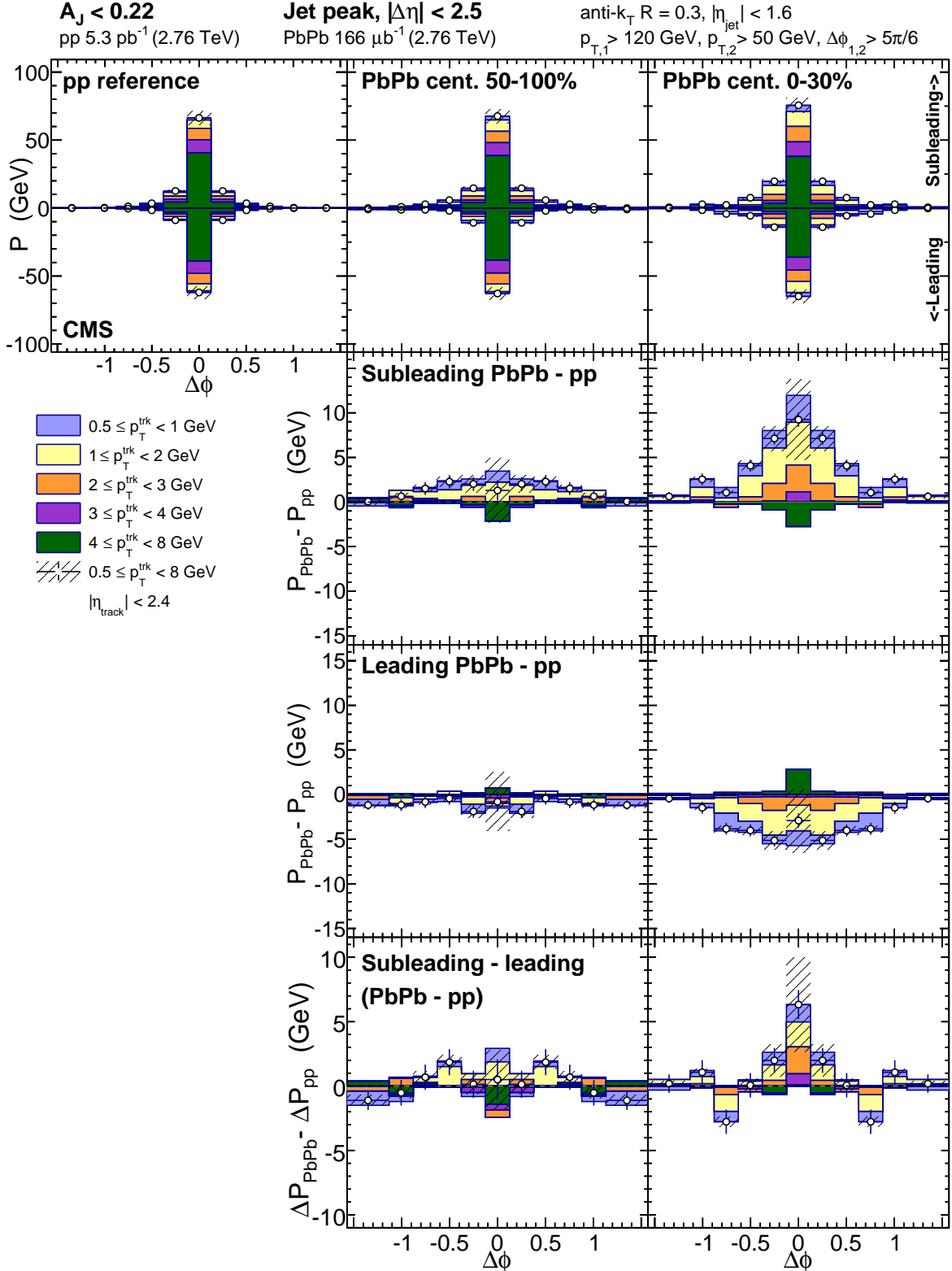


Figure 6: Top row: jet-peak (long-range subtracted) distribution in $\Delta\phi$ of p_T^{trk} about the sub-leading (plotted positive) and leading (plotted negative) jets for balanced dijet events with $A_J < 0.22$. Middle rows: PbPb-pp momentum distribution differences for subleading and leading jets. Bottom row: PbPb-pp, subleading-leading double difference in these $\Delta\phi$ momentum distributions. Statistical uncertainties are shown with vertical bars, and systematic uncertainties are shown with shaded boxes.

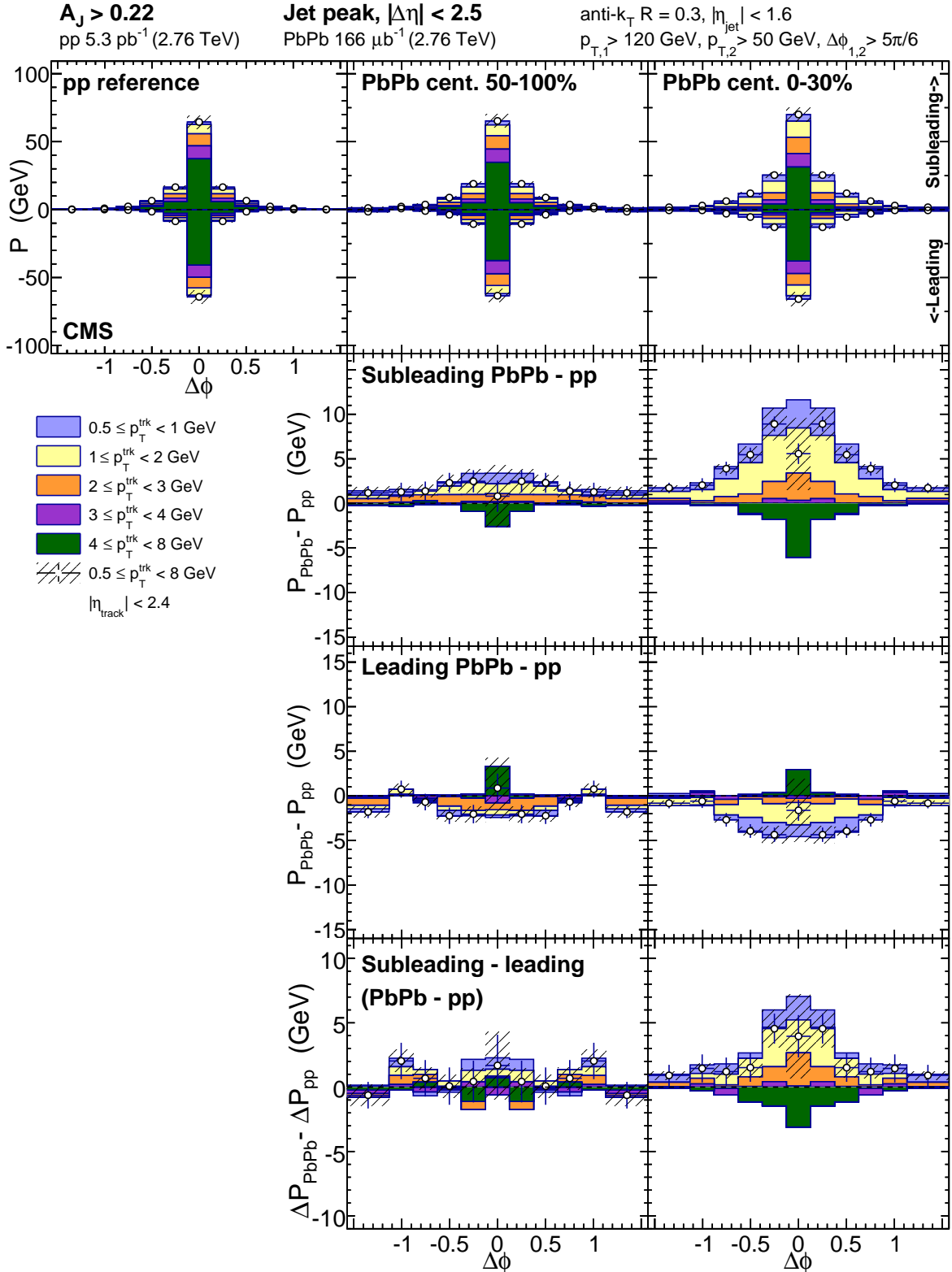


Figure 7: Top row: jet-peak (long-range subtracted) distribution in $\Delta\phi$ of p_T^{trk} about the sub-leading (plotted positive) and leading (plotted negative) jets for unbalanced dijet events with $A_J > 0.22$. Middle rows: PbPb-pp momentum distribution differences for subleading and leading jets. Bottom row: PbPb-pp, subleading-leading double difference in these $\Delta\phi$ momentum distributions. Statistical uncertainties are shown with vertical bars, and systematic uncertainties are shown with shaded boxes.

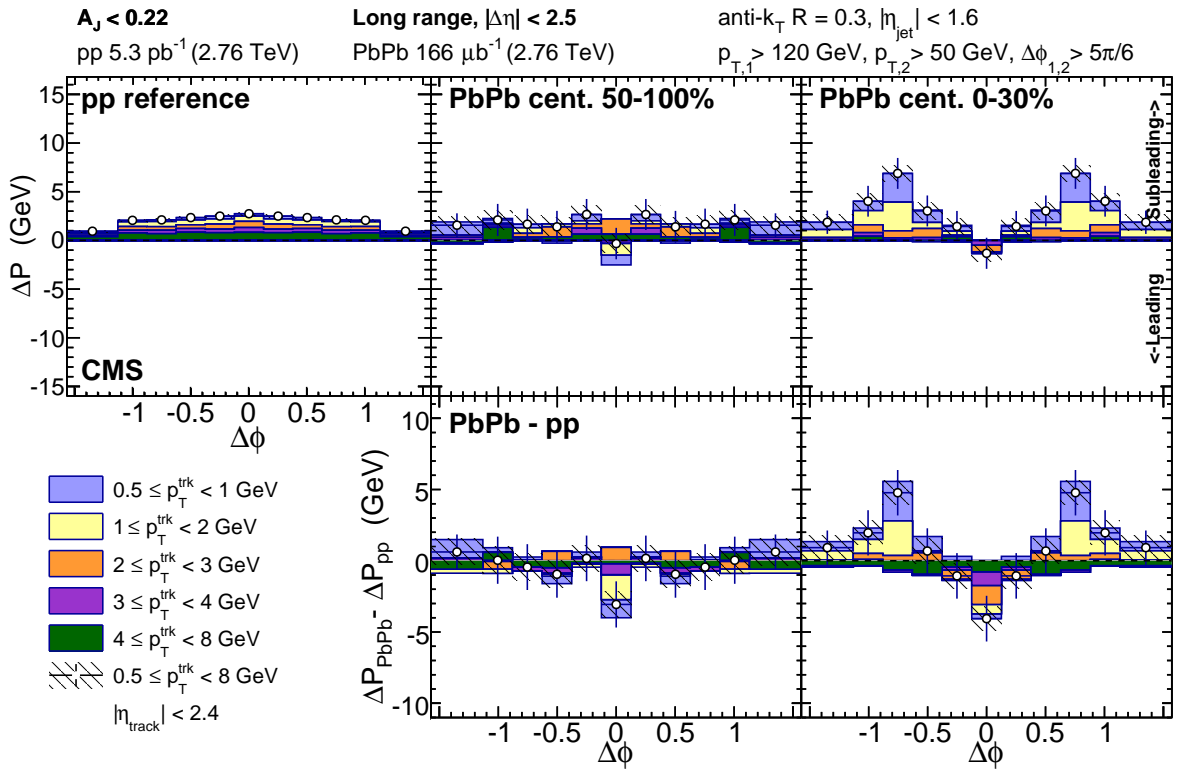


Figure 8: Top row: long-range distribution in $\Delta\phi$ of excess p_T^{trk} in the subleading relative to leading sides for balanced dijet events with $A_J < 0.22$. Bottom row: PbPb–pp difference in these $\Delta\phi$ long-range momentum distributions. Statistical uncertainties are shown with vertical bars, and systematic uncertainties are shown with shaded boxes.

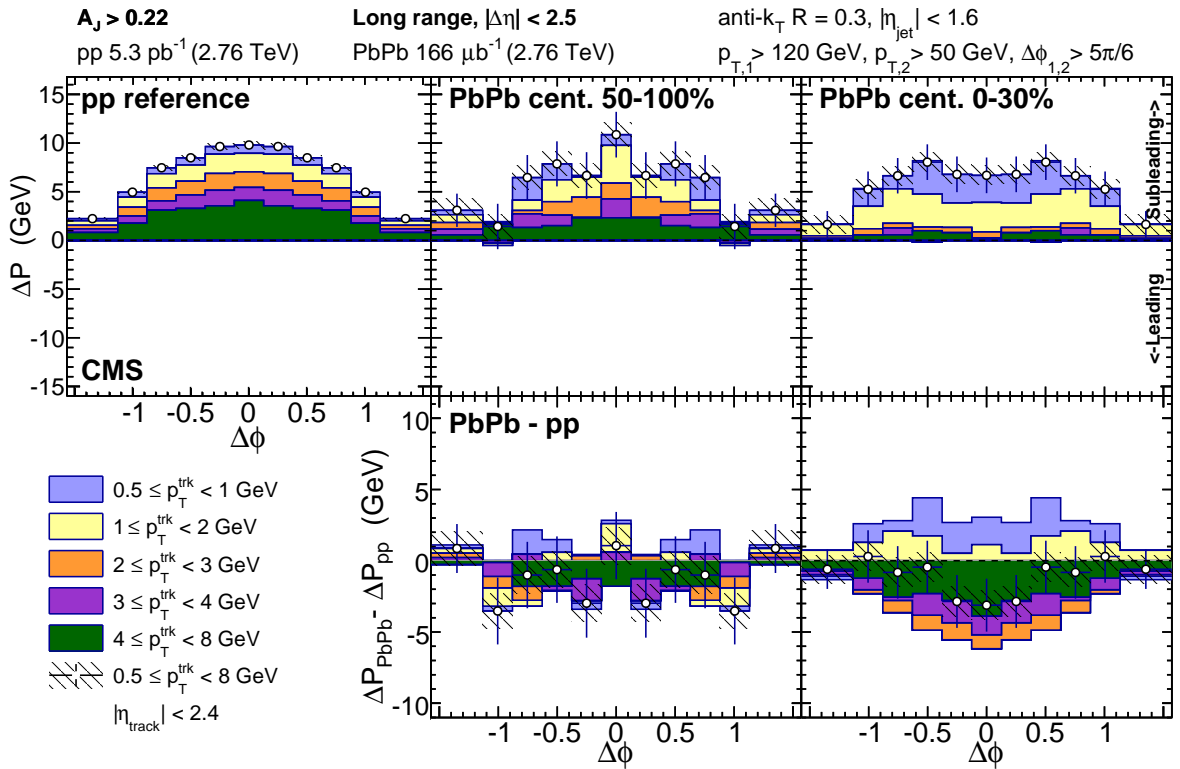


Figure 9: Top row: long-range distribution in $\Delta\phi$ of excess p_T^{trk} in the subleading relative to leading sides for unbalanced dijet events with $A_J > 0.22$. Bottom row: PbPb–pp difference in these $\Delta\phi$ long-range momentum distributions. Statistical uncertainties are shown with vertical bars, and systematic uncertainties are shown with shaded boxes.

6.3 Integrated hemisphere momentum balance

To summarize all contributions to the overall p_T^{trk} flow in the dijet events, we first present the hemisphere integral $\Sigma\Delta P$ (where ΔP represents the subleading-to-leading difference in the $\Delta\phi$ distribution of p_T^{trk} in the event) for this long-range asymmetry, measured in $|\Delta\phi| < \pi/2$ and $|\Delta\eta| < 2.5$, in Fig. 10. For balanced dijet events, the PbPb and pp integrals follow similar p_T^{trk} dependences. For unbalanced dijet events, the overall asymmetry rises with p_T^{trk} in the pp reference data, but falls with p_T^{trk} in central PbPb data, indicating the presence of different sources for the long-range momentum correlations. Finally, a summary of hemisphere-integrated excess (PbPb–pp) yields from all assessed sources for balanced and unbalanced dijet events is shown in Figs. 11 and 12. The top panels of Fig. 11 present total central PbPb–pp differences in p_T^{trk} associated with the subleading (plotted positive) and leading (plotted negative) jets. The leading and subleading jet peak modifications offset each other, so the total jet-peak-related modification, constructed from these two distributions, is also presented. The total jet peak modifications in central PbPb collisions are not significantly different in unbalanced versus balanced dijet events. The bottom panels of Fig. 11 present these jet-peak modifications together with the long-range modifications evident in Fig. 10 to show the decomposed hemisphere-wide differences in associated p_T in each track p_T range. Unlike the jet peak contributions, the long-range PbPb versus pp modifications are greater than their uncertainties between balanced and unbalanced dijet events. Here the depletion of high- p_T tracks in unbalanced PbPb versus pp dijet events corresponds to the reduced contribution from additional jets (which are prominently evident in the long-range distribution for pp unbalanced dijet events) in central PbPb unbalanced dijet events. Figure 12 presents the same hemisphere-integrated PbPb–pp excess for peripheral collisions for comparison to the central results shown in Fig. 11. Some possible small modifications are already evident in this 50–100% centrality range, but these differences between peripheral PbPb and pp results are in most cases smaller than systematic uncertainties.

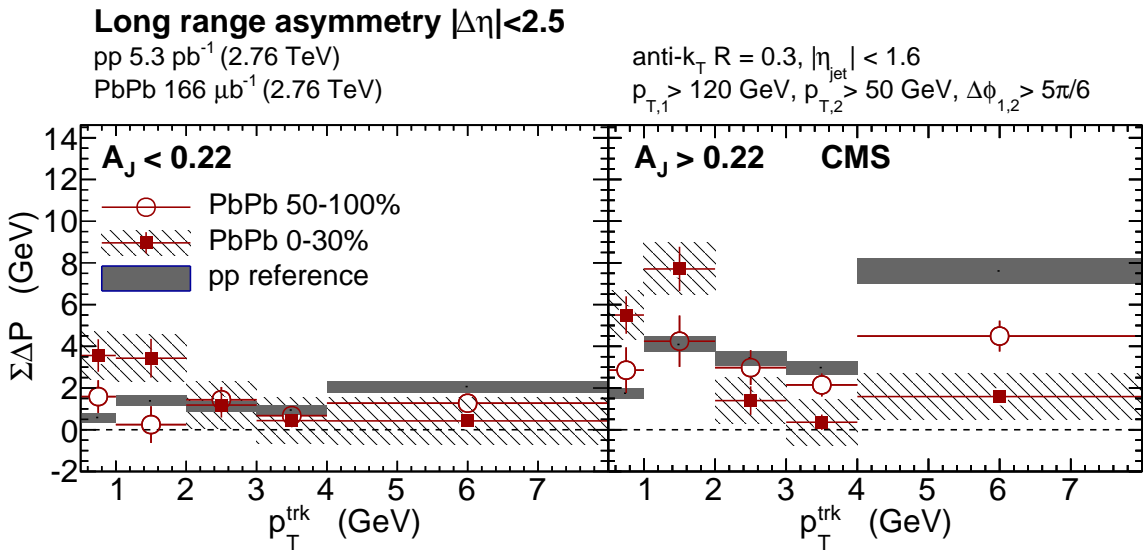


Figure 10: Integrated p_T in the long-range $\Delta\phi$ -correlated distribution as a function of track- p_T^{trk} integrated over $|\Delta\phi| < \pi/2$ and $|\Delta\eta| < 2.5$ for pp reference, peripheral PbPb and central PbPb data for balanced compared to unbalanced dijet events. Statistical uncertainties are shown with vertical bars, and systematic uncertainties are shown with shaded boxes.

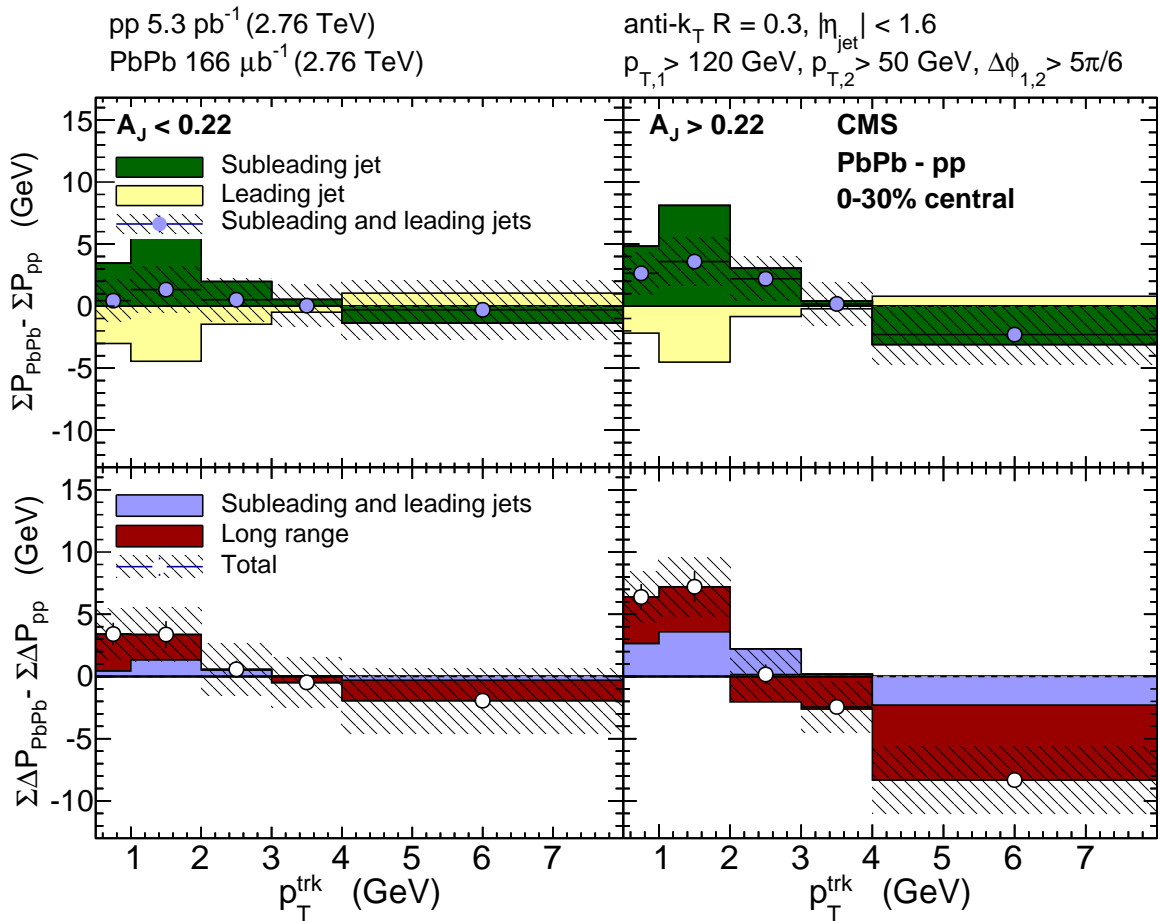


Figure 11: Modifications of jet-track correlated p_T^{trk} in central PbPb collisions with respect to the pp reference data, integrated over $|\Delta\phi| < \pi/2$ and $|\Delta\eta| < 2.5$. Top row: subleading and leading jet peaks PbPb–pp. Bottom row: relative contributions from jet peaks and long-range asymmetry to the double difference (PbPb–pp, subleading–leading) in total hemisphere p_T^{trk} . Statistical uncertainties are shown with vertical bars, and systematic uncertainties are shown with shaded boxes.

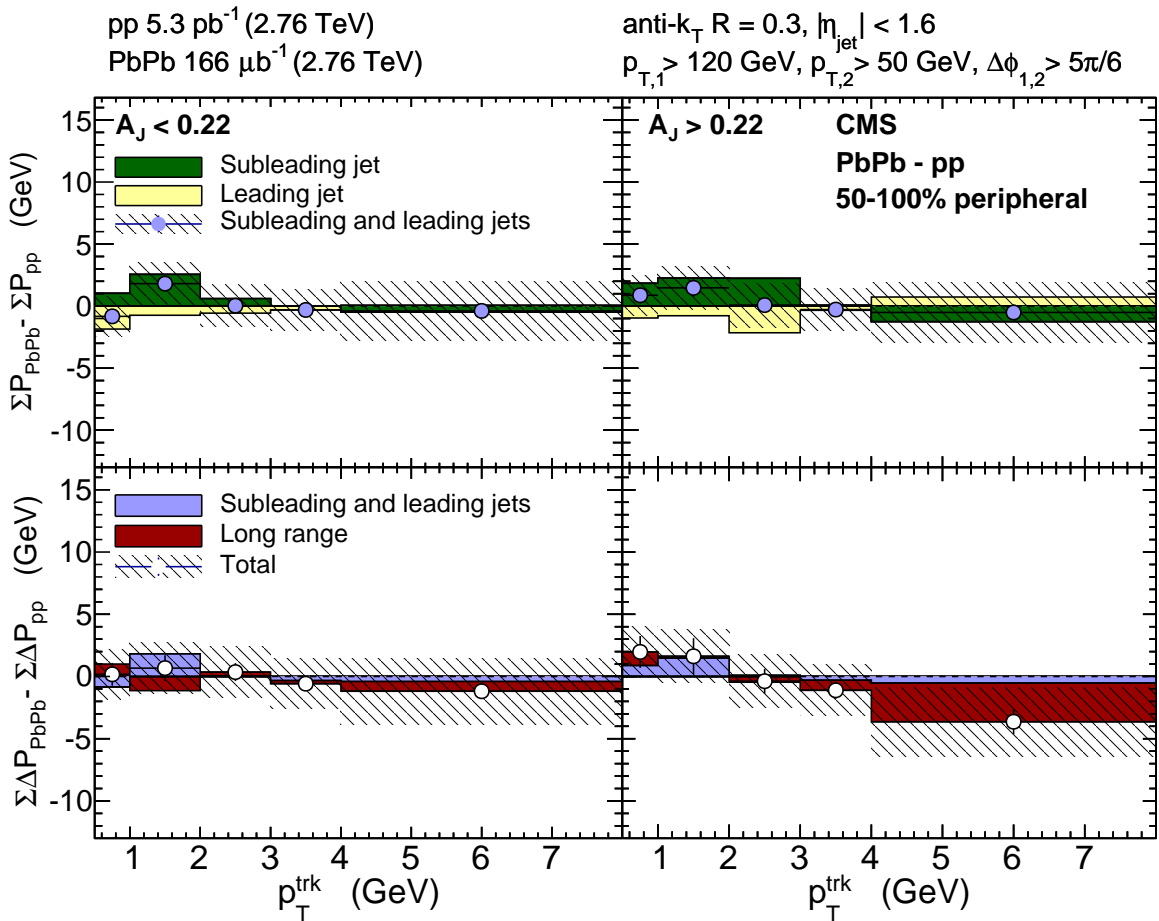


Figure 12: Modifications of jet-track correlated p_T^{trk} in peripheral PbPb collisions with respect to the pp reference data, integrated over $|\Delta\phi| < \pi/2$ and $|\Delta\eta| < 2.5$. Top row: subleading and leading jet peaks PbPb-pp. Bottom row: relative contributions from jet peaks and two-dimensional asymmetry to the double difference PbPb-pp, subleading-leading in total hemisphere p_T^{trk} . Statistical uncertainties are shown with vertical bars, and systematic uncertainties are shown with shaded boxes.

7 Summary

In this analysis, the redistribution of momentum in dijet events is studied via two-dimensional $\Delta\eta$ - $\Delta\phi$ jet-track correlations in PbPb and pp collisions at $\sqrt{s_{\text{NN}}} = 2.76$ TeV, using data sets with integrated luminosities of $166 \mu\text{b}^{-1}$ and 5.3 pb^{-1} , respectively. Events are selected to include a leading jet with $p_{\text{T},1} > 120 \text{ GeV}$ and subleading jet with $p_{\text{T},2} > 50 \text{ GeV}$, with an azimuthal separation of at least $\Delta\phi_{1,2} > 5\pi/6$. Subtracting the long-range part of the correlation from the jet peaks, this work extends the studies of jet shape modifications in PbPb events relative to pp collisions to large radial distances ($\Delta r \approx 1$) from the jet axis. These modifications are found to extend out to the largest radial distance studied in central PbPb events for both leading and subleading jets. The jet modifications are further studied differentially for balanced and unbalanced dijet events, and as a function of $p_{\text{T}}^{\text{trk}}$ and collision centrality for each of these selections in PbPb and pp reference data. Transverse momentum redistribution around the subleading and leading jets, as well as differences in long-range correlated background asymmetry, are separately analyzed.

An excess of transverse momentum carried by soft particles ($p_{\text{T}}^{\text{trk}} < 2 \text{ GeV}$) is found for both leading and subleading jets in central PbPb collisions relative to the pp reference, consistent with previous studies of charged-particle yields correlated to high- p_{T} jets. For unbalanced dijet events, this low- $p_{\text{T}}^{\text{trk}}$ excess is greater on the subleading-jet side than on the leading-jet side. However, the difference in $p_{\text{T}}^{\text{trk}}$ contained in the Gaussian-like jet peaks is found only partially to account for the total $p_{\text{T}}^{\text{trk}}$ redistribution in the most central PbPb collisions with dijet events. In the long-range correlated distribution of $p_{\text{T}}^{\text{trk}}$ under the jet peaks, it is found that the excess of relatively high- p_{T} particles ($2 < p_{\text{T}}^{\text{trk}} < 8 \text{ GeV}$) on the subleading side relative to the leading side, which is observed in asymmetric pp collisions and mainly attributed to three-jet events, is absent in most central PbPb collisions. This indicates that the fraction of events with additional jets in the asymmetric dijet sample is significantly lower than in an identical selection of dijet events in pp data. A long-range asymmetry in the low- p_{T} particles in dijet events is also observed, providing further input for the theoretical understanding of jet-medium coupling.

Acknowledgments

We congratulate our colleagues in the CERN accelerator departments for the excellent performance of the LHC and thank the technical and administrative staffs at CERN and at other CMS institutes for their contributions to the success of the CMS effort. In addition, we gratefully acknowledge the computing centres and personnel of the Worldwide LHC Computing Grid for delivering so effectively the computing infrastructure essential to our analyses. Finally, we acknowledge the enduring support for the construction and operation of the LHC and the CMS detector provided by the following funding agencies: BMWFW and FWF (Austria); FNRS and FWO (Belgium); CNPq, CAPES, FAPERJ, and FAPESP (Brazil); MES (Bulgaria); CERN; CAS, MoST, and NSFC (China); COLCIENCIAS (Colombia); MSES and CSF (Croatia); RPF (Cyprus); SENESCYT (Ecuador); MoER, ERC IUT and ERDF (Estonia); Academy of Finland, MEC, and HIP (Finland); CEA and CNRS/IN2P3 (France); BMBF, DFG, and HGF (Germany); GSRT (Greece); OTKA and NIH (Hungary); DAE and DST (India); IPM (Iran); SFI (Ireland); INFN (Italy); MSIP and NRF (Republic of Korea); LAS (Lithuania); MOE and UM (Malaysia); BUAP, CINVESTAV, CONACYT, LNS, SEP, and UASLP-FAI (Mexico); MBIE (New Zealand); PAEC (Pakistan); MSHE and NSC (Poland); FCT (Portugal); JINR (Dubna); MON, RosAtom, RAS and RFBR (Russia); MESTD (Serbia); SEIDI and CPAN (Spain); Swiss Funding Agencies (Switzerland); MST (Taipei); ThEPCenter, IPST, STAR and NSTDA (Thailand); TUBITAK and TAEK (Turkey); NASU and SFFR (Ukraine); STFC (United Kingdom); DOE and NSF (USA).

Individuals have received support from the Marie-Curie programme and the European Research Council and EPLANET (European Union); the Leventis Foundation; the A. P. Sloan Foundation; the Alexander von Humboldt Foundation; the Belgian Federal Science Policy Office; the Fonds pour la Formation à la Recherche dans l'Industrie et dans l'Agriculture (FRIA-Belgium); the Agentschap voor Innovatie door Wetenschap en Technologie (IWT-Belgium); the Ministry of Education, Youth and Sports (MEYS) of the Czech Republic; the Council of Science and Industrial Research, India; the HOMING PLUS programme of the Foundation for Polish Science, cofinanced from European Union, Regional Development Fund, the Mobility Plus programme of the Ministry of Science and Higher Education, the National Science Center (Poland), contracts Harmonia 2014/14/M/ST2/00428, Opus 2013/11/B/ST2/04202, 2014/13/B/ST2/02543 and 2014/15/B/ST2/03998, Sonata-bis 2012/07/E/ST2/01406; the Thalis and Aristeia programmes cofinanced by EU-ESF and the Greek NSRF; the National Priorities Research Program by Qatar National Research Fund; the Programa Clarín-COFUND del Principado de Asturias; the Rachadapisek Sompot Fund for Postdoctoral Fellowship, Chulalongkorn University and the Chulalongkorn Academic into Its 2nd Century Project Advancement Project (Thailand); and the Welch Foundation, contract C-1845.

References

- [1] J. D. Bjorken, “Energy loss of energetic partons in QGP: possible extinction of high p_T jets in hadron-hadron collisions”, (1982). FERMILAB-PUB-82-059-THY.
- [2] STAR Collaboration, “Direct observation of dijets in central Au+Au collisions at $\sqrt{s_{\text{NN}}} = 200 \text{ GeV}$ ”, *Phys. Rev. Lett.* **97** (2006) 162301,
[doi:10.1103/PhysRevLett.97.162301](https://doi.org/10.1103/PhysRevLett.97.162301), arXiv:[nucl-ex/0604018](https://arxiv.org/abs/nucl-ex/0604018).
- [3] PHENIX Collaboration, “Transverse momentum and centrality dependence of dihadron correlations in Au+Au collisions at $\sqrt{s_{\text{NN}}} = 200 \text{ GeV}$: Jet-quenching and the response of partonic matter”, *Phys. Rev. C* **77** (2008) 011901,
[doi:10.1103/PhysRevC.77.011901](https://doi.org/10.1103/PhysRevC.77.011901), arXiv:[0705.3238](https://arxiv.org/abs/0705.3238).

- [4] ATLAS Collaboration, “Observation of a Centrality-Dependent Dijet Asymmetry in Lead-Lead Collisions at $\sqrt{s_{\text{NN}}} = 2.76$ TeV with the ATLAS Detector at the LHC”, *Phys. Rev. Lett.* **105** (2010) 252303, doi:10.1103/PhysRevLett.105.252303, arXiv:1011.6182.
- [5] CMS Collaboration, “Observation and studies of jet quenching in PbPb collisions at $\sqrt{s_{\text{NN}}} = 2.76$ TeV”, *Phys. Rev. C* **84** (2011) 024906, doi:10.1103/PhysRevC.84.024906, arXiv:1102.1957.
- [6] CMS Collaboration, “Jet momentum dependence of jet quenching in PbPb collisions at $\sqrt{s_{\text{NN}}} = 2.76$ TeV”, *Phys. Lett. B* **712** (2012) 176, doi:10.1016/j.physletb.2012.04.058, arXiv:1202.5022.
- [7] ALICE Collaboration, “Measurement of jet suppression in central Pb-Pb collisions at $\sqrt{s_{\text{NN}}} = 2.76$ TeV”, *Phys. Lett. B* **746** (2015) 1, doi:10.1016/j.physletb.2015.04.039, arXiv:1502.01689.
- [8] CMS Collaboration, “Studies of dijet transverse momentum balance and pseudorapidity distributions in pPb collisions at $\sqrt{s_{\text{NN}}} = 5.02$ TeV”, *Eur. Phys. J. C.* **74** (2014) 2951, doi:10.1140/epjc/s10052-014-2951-y, arXiv:1401.4433.
- [9] CMS Collaboration, “Measurement of transverse momentum relative to dijet systems in PbPb and pp collisions at $\sqrt{s_{\text{NN}}} = 2.76$ TeV”, *JHEP* **01** (2016) 6, doi:10.1007/JHEP01(2016)006, arXiv:1509.09029.
- [10] CMS Collaboration, “Measurement of jet fragmentation in PbPb and pp collisions at $\sqrt{s_{\text{NN}}} = 2.76$ TeV”, *Phys. Rev. C* **90** (2014) 024908, doi:10.1103/PhysRevC.90.024908, arXiv:1406.0932.
- [11] CMS Collaboration, “Modification of jet shapes in PbPb collisions at $\sqrt{s_{\text{NN}}} = 2.76$ TeV”, *Phys. Lett. B* **730** (2014) 243, doi:10.1016/j.physletb.2014.01.042, arXiv:1310.0878.
- [12] CMS Collaboration, “Correlations between jets and charged particles in PbPb and pp collisions at $\sqrt{s_{\text{NN}}} = 2.76$ TeV”, *JHEP* **02** (2016) 156, doi:10.1007/JHEP02(2016)156, arXiv:1601.00079.
- [13] CMS Collaboration, “Determination of Jet Energy Calibration and Transverse Momentum Resolution in CMS”, *JINST* **6** (2011) P11002, doi:10.1088/1748-0221/6/11/P11002, arXiv:1107.4277.
- [14] CMS Collaboration, “Description and performance of track and primary-vertex reconstruction with the CMS tracker”, *JINST* **9** (2014) P10009, doi:10.1088/1748-0221/9/10/P10009, arXiv:1405.6569.
- [15] CMS Collaboration, “The CMS experiment at the CERN LHC”, *JINST* **3** (2008) S08004, doi:10.1088/1748-0221/3/08/S08004.
- [16] M. Cacciari, G. P. Salam, and G. Soyez, “FastJet user manual”, *Eur. Phys. J. C* **72** (2012) 1896, doi:10.1140/epjc/s10052-012-1896-2, arXiv:1111.6097.
- [17] M. Cacciari, G. P. Salam, and G. Soyez, “The anti- k_t jet clustering algorithm”, *JHEP* **04** (2008) 063, doi:10.1088/1126-6708/2008/04/063, arXiv:0802.1189.

- [18] CMS Collaboration, “Underlying-Event Subtraction for Particle Flow”, CMS Detector Performance Summary CMS-DP-2013-018, 2013.
- [19] T. Sjöstrand, S. Mrenna, and P. Skands, “PYTHIA 6.4 physics and manual”, *JHEP* **05** (2006) 026, doi:10.1088/1126-6708/2006/05/026, arXiv:hep-ph/0603175.
- [20] R. Field, “Early LHC Underlying Event Data - Findings and Surprises”, in *Hadron collider physics. Proceedings, 22nd Conference, HCP 2010, Toronto, Canada*. 2010. arXiv:1010.3558.
- [21] GEANT4 Collaboration, “GEANT4 — a simulation toolkit”, *Nucl. Instrum. Meth. A* **506** (2003) 250, doi:10.1016/S0168-9002(03)01368-8.
- [22] I. P. Lokhtin and A. M. Snigirev, “A model of jet quenching in ultrarelativistic heavy ion collisions and high- p_T hadron spectra at RHIC”, *Eur. Phys. J. C* **45** (2006) 211, doi:10.1140/epjc/s2005-02426-3, arXiv:hep-ph/0506189.
- [23] CMS Collaboration, “Study of high- p_T charged particle suppression in PbPb compared to pp collisions at $\sqrt{s_{NN}} = 2.76$ TeV”, *Eur. Phys. J. C* **72** (2012) 1945, doi:10.1140/epjc/s10052-012-1945-x, arXiv:1202.2554.
- [24] CMS Collaboration, “The CMS high level trigger”, *Eur. Phys. J. C* **46** (2006) 605, doi:10.1140/epjc/s2006-02495-8, arXiv:hep-ex/0512077.
- [25] CMS Collaboration, “Studies of jet quenching using isolated-photon+jet correlations in PbPb and pp collisions at $\sqrt{s_{NN}} = 2.76$ TeV”, *Phys. Lett. B* **718** (2013) 773, doi:10.1016/j.physletb.2012.11.003, arXiv:1205.0206.
- [26] CMS Collaboration, “Multiplicity and transverse momentum dependence of two- and four-particle correlations in pPb and PbPb collisions”, *Phys. Lett. B* **724** (2013) 213, doi:10.1016/j.physletb.2013.06.028, arXiv:1305.0609.
- [27] CMS Collaboration, “Observation of long-range, near-side angular correlations in proton-proton collisions at the LHC”, *JHEP* **09** (2010) 091, doi:10.1007/JHEP09(2010)091, arXiv:1009.4122.
- [28] CMS Collaboration, “Long-range and short-range dihadron angular correlations in central PbPb collisions at $\sqrt{s_{NN}} = 2.76$ TeV”, *JHEP* **07** (2011) 076, doi:10.1007/JHEP07(2011)076.
- [29] CMS Collaboration, “Observation of long-range, near-side angular correlations in pPb collisions at the LHC.”, *Phys. Lett. B* **718** (2013) 795, doi:10.1016/j.physletb.2012.11.025, arXiv:1210.5482.
- [30] CMS Collaboration, “Measurement of higher-order harmonic azimuthal anisotropy in PbPb collisions at $\sqrt{s_{NN}} = 2.76$ TeV”, *Phys. Rev. C* **89** (2014) 044906, doi:10.1103/PhysRevC.89.044906, arXiv:1310.8651.
- [31] G.-Y. Qin and X.-N. Wang, “Jet quenching in high-energy heavy-ion collisions”, *Mod. Phys. E* **24** (2015) 1530014, doi:10.1142/S0218301315300143, arXiv:1511.00790.

A The CMS Collaboration

Yerevan Physics Institute, Yerevan, Armenia
V. Khachatryan, A.M. Sirunyan, A. Tumasyan

Institut für Hochenergiephysik der OeAW, Wien, Austria

W. Adam, E. Asilar, T. Bergauer, J. Brandstetter, E. Brondolin, M. Dragicevic, J. Erö, M. Flechl, M. Friedl, R. Frühwirth¹, V.M. Ghete, C. Hartl, N. Hörmann, J. Hrubec, M. Jeitler¹, A. König, I. Krätschmer, D. Liko, T. Matsushita, I. Mikulec, D. Rabady, N. Rad, B. Rahbaran, H. Rohringer, J. Schieck¹, J. Strauss, W. Treberer-Treberspurg, W. Waltenberger, C.-E. Wulz¹

National Centre for Particle and High Energy Physics, Minsk, Belarus

V. Mossolov, N. Shumeiko, J. Suarez Gonzalez

Universiteit Antwerpen, Antwerpen, Belgium

S. Alderweireldt, E.A. De Wolf, X. Janssen, J. Lauwers, M. Van De Klundert, H. Van Haevermaet, P. Van Mechelen, N. Van Remortel, A. Van Spilbeeck

Vrije Universiteit Brussel, Brussel, Belgium

S. Abu Zeid, F. Blekman, J. D'Hondt, N. Daci, I. De Bruyn, K. Deroover, N. Heracleous, S. Lowette, S. Moortgat, L. Moreels, A. Olbrechts, Q. Python, S. Tavernier, W. Van Doninck, P. Van Mulders, I. Van Parijs

Université Libre de Bruxelles, Bruxelles, Belgium

H. Brun, C. Caillol, B. Clerbaux, G. De Lentdecker, H. Delannoy, G. Fasanella, L. Favart, R. Goldouzian, A. Grebenyuk, G. Karapostoli, T. Lenzi, A. Léonard, J. Luetic, T. Maerschalk, A. Marinov, A. Randle-conde, T. Seva, C. Vander Velde, P. Vanlaer, R. Yonamine, F. Zenoni, F. Zhang²

Ghent University, Ghent, Belgium

A. Cimmino, T. Cornelis, D. Dobur, A. Fagot, G. Garcia, M. Gul, D. Poyraz, S. Salva, R. Schöfbeck, M. Tytgat, W. Van Driessche, E. Yazgan, N. Zaganidis

Université Catholique de Louvain, Louvain-la-Neuve, Belgium

H. Bakhshiansohi, C. Beluffi³, O. Bondu, S. Brochet, G. Bruno, A. Caudron, S. De Visscher, C. Delaere, M. Delcourt, L. Forthomme, B. Francois, A. Giannanco, A. Jafari, P. Jez, M. Komm, V. Lemaitre, A. Magitteri, A. Mertens, M. Musich, C. Nuttens, K. Piotrkowski, L. Quertenmont, M. Selvaggi, M. Vidal Marono, S. Wertz

Université de Mons, Mons, Belgium

N. Belyi

Centro Brasileiro de Pesquisas Fisicas, Rio de Janeiro, Brazil

W.L. Aldá Júnior, F.L. Alves, G.A. Alves, L. Brito, C. Hensel, A. Moraes, M.E. Pol, P. Rebello Teles

Universidade do Estado do Rio de Janeiro, Rio de Janeiro, Brazil

E. Belchior Batista Das Chagas, W. Carvalho, J. Chinellato⁴, A. Custódio, E.M. Da Costa, G.G. Da Silveira⁵, D. De Jesus Damiao, C. De Oliveira Martins, S. Fonseca De Souza, L.M. Huertas Guativa, H. Malbouisson, D. Matos Figueiredo, C. Mora Herrera, L. Mundim, H. Nogima, W.L. Prado Da Silva, A. Santoro, A. Sznajder, E.J. Tonelli Manganote⁴, A. Vilela Pereira

Universidade Estadual Paulista ^a, Universidade Federal do ABC ^b, São Paulo, Brazil

S. Ahuja^a, C.A. Bernardes^b, S. Dogra^a, T.R. Fernandez Perez Tomei^a, E.M. Gregores^b,

P.G. Mercadante^b, C.S. Moon^a, S.F. Novaes^a, Sandra S. Padula^a, D. Romero Abad^b, J.C. Ruiz Vargas

Institute for Nuclear Research and Nuclear Energy, Sofia, Bulgaria

A. Aleksandrov, R. Hadjiiska, P. Iaydjiev, M. Rodozov, S. Stoykova, G. Sultanov, M. Vutova

University of Sofia, Sofia, Bulgaria

A. Dimitrov, I. Glushkov, L. Litov, B. Pavlov, P. Petkov

Beihang University, Beijing, China

W. Fang⁶

Institute of High Energy Physics, Beijing, China

M. Ahmad, J.G. Bian, G.M. Chen, H.S. Chen, M. Chen, Y. Chen⁷, T. Cheng, C.H. Jiang, D. Leggat, Z. Liu, F. Romeo, S.M. Shaheen, A. Spiezia, J. Tao, C. Wang, Z. Wang, H. Zhang, J. Zhao

State Key Laboratory of Nuclear Physics and Technology, Peking University, Beijing, China

Y. Ban, G. Chen, Q. Li, S. Liu, Y. Mao, S.J. Qian, D. Wang, Z. Xu

Universidad de Los Andes, Bogota, Colombia

C. Avila, A. Cabrera, L.F. Chaparro Sierra, C. Florez, J.P. Gomez, C.F. González Hernández, J.D. Ruiz Alvarez, J.C. Sanabria

University of Split, Faculty of Electrical Engineering, Mechanical Engineering and Naval Architecture, Split, Croatia

N. Godinovic, D. Lelas, I. Puljak, P.M. Ribeiro Cipriano

University of Split, Faculty of Science, Split, Croatia

Z. Antunovic, M. Kovac

Institute Rudjer Boskovic, Zagreb, Croatia

V. Brigljevic, D. Ferencek, K. Kadija, S. Micanovic, L. Sudic, T. Susa

University of Cyprus, Nicosia, Cyprus

A. Attikis, G. Mavromanolakis, J. Mousa, C. Nicolaou, F. Ptochos, P.A. Razis, H. Rykaczewski

Charles University, Prague, Czech Republic

M. Finger⁸, M. Finger Jr.⁸

Universidad San Francisco de Quito, Quito, Ecuador

E. Carrera Jarrin

Academy of Scientific Research and Technology of the Arab Republic of Egypt, Egyptian Network of High Energy Physics, Cairo, Egypt

A. Ellithi Kamel⁹, M.A. Mahmoud^{10,11}, A. Radi^{11,12}

National Institute of Chemical Physics and Biophysics, Tallinn, Estonia

B. Calpas, M. Kadastik, M. Murumaa, L. Perrini, M. Raidal, A. Tiko, C. Veelken

Department of Physics, University of Helsinki, Helsinki, Finland

P. Eerola, J. Pekkanen, M. Voutilainen

Helsinki Institute of Physics, Helsinki, Finland

J. Hätkönen, V. Karimäki, R. Kinnunen, T. Lampén, K. Lassila-Perini, S. Lehti, T. Lindén, P. Luukka, T. Peltola, J. Tuominiemi, E. Tuovinen, L. Wendland

Lappeenranta University of Technology, Lappeenranta, Finland

J. Talvitie, T. Tuuva

IRFU, CEA, Université Paris-Saclay, Gif-sur-Yvette, France

M. Besancon, F. Couderc, M. Dejardin, D. Denegri, B. Fabbro, J.L. Faure, C. Favaro, F. Ferri, S. Ganjour, S. Ghosh, A. Givernaud, P. Gras, G. Hamel de Monchenault, P. Jarry, I. Kucher, E. Locci, M. Machet, J. Rander, A. Rosowsky, M. Titov, A. Zghiche

Laboratoire Leprince-Ringuet, Ecole Polytechnique, IN2P3-CNRS, Palaiseau, France

A. Abdulsalam, I. Antropov, S. Baffioni, F. Beaudette, P. Busson, L. Cadamuro, E. Chapon, C. Charlot, O. Davignon, R. Granier de Cassagnac, M. Jo, S. Lisniak, P. Miné, M. Nguyen, C. Ochando, G. Ortona, P. Paganini, P. Pigard, S. Regnard, R. Salerno, Y. Sirois, T. Strebler, Y. Yilmaz, A. Zabi

Institut Pluridisciplinaire Hubert Curien, Université de Strasbourg, Université de Haute Alsace Mulhouse, CNRS/IN2P3, Strasbourg, France

J.-L. Agram¹³, J. Andrea, A. Aubin, D. Bloch, J.-M. Brom, M. Buttignol, E.C. Chabert, N. Chanon, C. Collard, E. Conte¹³, X. Coubez, J.-C. Fontaine¹³, D. Gelé, U. Goerlach, A.-C. Le Bihan, J.A. Merlin¹⁴, K. Skovpen, P. Van Hove

Centre de Calcul de l’Institut National de Physique Nucléaire et de Physique des Particules, CNRS/IN2P3, Villeurbanne, France

S. Gadrat

Université de Lyon, Université Claude Bernard Lyon 1, CNRS-IN2P3, Institut de Physique Nucléaire de Lyon, Villeurbanne, France

S. Beauceron, C. Bernet, G. Boudoul, E. Bouvier, C.A. Carrillo Montoya, R. Chierici, D. Contardo, B. Courbon, P. Depasse, H. El Mamouni, J. Fan, J. Fay, S. Gascon, M. Gouzevitch, G. Grenier, B. Ille, F. Lagarde, I.B. Laktineh, M. Lethuillier, L. Mirabito, A.L. Pequegnot, S. Perries, A. Popov¹⁵, D. Sabes, V. Sordini, M. Vander Donckt, P. Verdier, S. Viret

Georgian Technical University, Tbilisi, Georgia

T. Toriashvili¹⁶

Tbilisi State University, Tbilisi, Georgia

Z. Tsamalaidze⁸

RWTH Aachen University, I. Physikalisches Institut, Aachen, Germany

C. Autermann, S. Beranek, L. Feld, A. Heister, M.K. Kiesel, K. Klein, M. Lipinski, A. Ostapchuk, M. Preuten, F. Raupach, S. Schael, C. Schomakers, J.F. Schulte, J. Schulz, T. Verlage, H. Weber, V. Zhukov¹⁵

RWTH Aachen University, III. Physikalisches Institut A, Aachen, Germany

M. Brodski, E. Dietz-Laursonn, D. Duchardt, M. Endres, M. Erdmann, S. Erdweg, T. Esch, R. Fischer, A. Güth, M. Hamer, T. Hebbeker, C. Heidemann, K. Hoepfner, S. Knutzen, M. Merschmeyer, A. Meyer, P. Millet, S. Mukherjee, M. Olschewski, K. Padeken, T. Pook, M. Radziej, H. Reithler, M. Rieger, F. Scheuch, L. Sonnenschein, D. Teyssier, S. Thüer

RWTH Aachen University, III. Physikalisches Institut B, Aachen, Germany

V. Cherepanov, G. Flügge, W. Haj Ahmad, F. Hoehle, B. Kargoll, T. Kress, A. Künsken, J. Lingemann, A. Nehrkorn, A. Nowack, I.M. Nugent, C. Pistone, O. Pooth, A. Stahl¹⁴

Deutsches Elektronen-Synchrotron, Hamburg, Germany

M. Aldaya Martin, C. Asawatangtrakuldee, K. Beernaert, O. Behnke, U. Behrens, A.A. Bin Anuar, K. Borras¹⁷, A. Campbell, P. Connor, C. Contreras-Campana, F. Costanza, C. Diez

Pardos, G. Dolinska, G. Eckerlin, D. Eckstein, E. Eren, E. Gallo¹⁸, J. Garay Garcia, A. Geiser, A. Gzhko, J.M. Grados Luyando, P. Gunnellini, A. Harb, J. Hauk, M. Hempel¹⁹, H. Jung, A. Kalogeropoulos, O. Karacheban¹⁹, M. Kasemann, J. Keaveney, J. Kieseler, C. Kleinwort, I. Korol, D. Krücker, W. Lange, A. Lelek, J. Leonard, K. Lipka, A. Lobanov, W. Lohmann¹⁹, R. Mankel, I.-A. Melzer-Pellmann, A.B. Meyer, G. Mittag, J. Mnich, A. Mussgiller, E. Ntomari, D. Pitzl, R. Placakyte, A. Raspereza, B. Roland, M.Ö. Sahin, P. Saxena, T. Schoerner-Sadenius, C. Seitz, S. Spannagel, N. Stefaniuk, K.D. Trippkewitz, G.P. Van Onsem, R. Walsh, C. Wissing

University of Hamburg, Hamburg, Germany

V. Blobel, M. Centis Vignali, A.R. Draeger, T. Dreyer, E. Garutti, D. Gonzalez, J. Haller, M. Hoffmann, A. Junkes, R. Klanner, R. Kogler, N. Kovalchuk, T. Lapsien, T. Lenz, I. Marchesini, D. Marconi, M. Meyer, M. Niedziela, D. Nowatschin, F. Pantaleo¹⁴, T. Peiffer, A. Perieanu, J. Poehlsen, C. Sander, C. Scharf, P. Schleper, A. Schmidt, S. Schumann, J. Schwandt, H. Stadie, G. Steinbrück, F.M. Stober, M. Stöver, H. Tholen, D. Troendle, E. Usai, L. Vanelderen, A. Vanhoefer, B. Vormwald

Institut für Experimentelle Kernphysik, Karlsruhe, Germany

C. Barth, C. Baus, J. Berger, E. Butz, T. Chwalek, F. Colombo, W. De Boer, A. Dierlamm, S. Fink, R. Friese, M. Giffels, A. Gilbert, P. Goldenzweig, D. Haitz, F. Hartmann¹⁴, S.M. Heindl, U. Husemann, I. Katkov¹⁵, P. Lobelle Pardo, B. Maier, H. Mildner, M.U. Mozer, T. Müller, Th. Müller, M. Plagge, G. Quast, K. Rabbertz, S. Röcker, F. Roscher, M. Schröder, I. Shvetsov, G. Sieber, H.J. Simonis, R. Ulrich, J. Wagner-Kuhr, S. Wayand, M. Weber, T. Weiler, S. Williamson, C. Wöhrmann, R. Wolf

Institute of Nuclear and Particle Physics (INPP), NCSR Demokritos, Aghia Paraskevi, Greece

G. Anagnostou, G. Daskalakis, T. Geralis, V.A. Giakoumopoulou, A. Kyriakis, D. Loukas, I. Topsis-Giotis

National and Kapodistrian University of Athens, Athens, Greece

A. Agapitos, S. Kesisoglou, A. Panagiotou, N. Saoulidou, E. Tziaferi

University of Ioánnina, Ioánnina, Greece

I. Evangelou, G. Flouris, C. Foudas, P. Kokkas, N. Loukas, N. Manthos, I. Papadopoulos, E. Paradas

MTA-ELTE Lendület CMS Particle and Nuclear Physics Group, Eötvös Loránd University, Budapest, Hungary

N. Filipovic

Wigner Research Centre for Physics, Budapest, Hungary

G. Bencze, C. Hajdu, P. Hidas, D. Horvath²⁰, F. Sikler, V. Veszpremi, G. Vesztergombi²¹, A.J. Zsigmond

Institute of Nuclear Research ATOMKI, Debrecen, Hungary

N. Beni, S. Czellar, J. Karancsi²², A. Makovec, J. Molnar, Z. Szillasi

University of Debrecen, Debrecen, Hungary

M. Bartók²¹, P. Raics, Z.L. Trocsanyi, B. Ujvari

National Institute of Science Education and Research, Bhubaneswar, India

S. Bahinipati, S. Choudhury²³, P. Mal, K. Mandal, A. Nayak²⁴, D.K. Sahoo, N. Sahoo, S.K. Swain

Panjab University, Chandigarh, India

S. Bansal, S.B. Beri, V. Bhatnagar, R. Chawla, U.Bhawandeep, A.K. Kalsi, A. Kaur, M. Kaur, R. Kumar, A. Mehta, M. Mittal, J.B. Singh, G. Walia

University of Delhi, Delhi, India

Ashok Kumar, A. Bhardwaj, B.C. Choudhary, R.B. Garg, S. Keshri, S. Malhotra, M. Naimuddin, N. Nishu, K. Ranjan, R. Sharma, V. Sharma

Saha Institute of Nuclear Physics, Kolkata, India

R. Bhattacharya, S. Bhattacharya, K. Chatterjee, S. Dey, S. Dutt, S. Dutta, S. Ghosh, N. Majumdar, A. Modak, K. Mondal, S. Mukhopadhyay, S. Nandan, A. Purohit, A. Roy, D. Roy, S. Roy Chowdhury, S. Sarkar, M. Sharan, S. Thakur

Indian Institute of Technology Madras, Madras, India

P.K. Behera

Bhabha Atomic Research Centre, Mumbai, India

R. Chudasama, D. Dutta, V. Jha, V. Kumar, A.K. Mohanty¹⁴, P.K. Netrakanti, L.M. Pant, P. Shukla, A. Topkar

Tata Institute of Fundamental Research-A, Mumbai, India

T. Aziz, S. Dugad, G. Kole, B. Mahakud, S. Mitra, G.B. Mohanty, B. Parida, N. Sur, B. Sutar

Tata Institute of Fundamental Research-B, Mumbai, India

S. Banerjee, S. Bhowmik²⁵, R.K. Dewanjee, S. Ganguly, M. Guchait, Sa. Jain, S. Kumar, M. Maity²⁵, G. Majumder, K. Mazumdar, T. Sarkar²⁵, N. Wickramage²⁶

Indian Institute of Science Education and Research (IISER), Pune, India

S. Chauhan, S. Dube, V. Hegde, A. Kapoor, K. Kothekar, A. Rane, S. Sharma

Institute for Research in Fundamental Sciences (IPM), Tehran, Iran

H. Behnamian, S. Chenarani²⁷, E. Eskandari Tadavani, S.M. Etesami²⁷, A. Fahim²⁸, M. Khakzad, M. Mohammadi Najafabadi, M. Naseri, S. Paktnat Mehdiabadi, F. Rezaei Hosseinabadi, B. Safarzadeh²⁹, M. Zeinali

University College Dublin, Dublin, Ireland

M. Felcini, M. Grunewald

INFN Sezione di Bari ^a, Università di Bari ^b, Politecnico di Bari ^c, Bari, Italy

M. Abbrescia^{a,b}, C. Calabria^{a,b}, C. Caputo^{a,b}, A. Colaleo^a, D. Creanza^{a,c}, L. Cristella^{a,b}, N. De Filippis^{a,c}, M. De Palma^{a,b}, L. Fiore^a, G. Iaselli^{a,c}, G. Maggi^{a,c}, M. Maggi^a, G. Miniello^{a,b}, S. My^{a,b}, S. Nuzzo^{a,b}, A. Pompili^{a,b}, G. Pugliese^{a,c}, R. Radogna^{a,b}, A. Ranieri^a, G. Selvaggi^{a,b}, L. Silvestris^{a,14}, R. Venditti^{a,b}, P. Verwilligen^a

INFN Sezione di Bologna ^a, Università di Bologna ^b, Bologna, Italy

G. Abbiendi^a, C. Battilana, D. Bonacorsi^{a,b}, S. Braibant-Giacomelli^{a,b}, L. Brigliadori^{a,b}, R. Campanini^{a,b}, P. Capiluppi^{a,b}, A. Castro^{a,b}, F.R. Cavallo^a, S.S. Chhibra^{a,b}, G. Codispoti^{a,b}, M. Cuffiani^{a,b}, G.M. Dallavalle^a, F. Fabbri^a, A. Fanfani^{a,b}, D. Fasanella^{a,b}, P. Giacomelli^a, C. Grandi^a, L. Guiducci^{a,b}, S. Marcellini^a, G. Masetti^a, A. Montanari^a, F.L. Navarria^{a,b}, A. Perrotta^a, A.M. Rossi^{a,b}, T. Rovelli^{a,b}, G.P. Siroli^{a,b}, N. Tosi^{a,b,14}

INFN Sezione di Catania ^a, Università di Catania ^b, Catania, Italy

S. Albergo^{a,b}, M. Chiorboli^{a,b}, S. Costa^{a,b}, A. Di Mattia^a, F. Giordano^{a,b}, R. Potenza^{a,b}, A. Tricomi^{a,b}, C. Tuve^{a,b}

INFN Sezione di Firenze ^a, Università di Firenze ^b, Firenze, Italy

G. Barbagli^a, V. Ciulli^{a,b}, C. Civinini^a, R. D'Alessandro^{a,b}, E. Focardi^{a,b}, V. Gori^{a,b}, P. Lenzi^{a,b}, M. Meschini^a, S. Paoletti^a, G. Sguazzoni^a, L. Viliani^{a,b,14}

INFN Laboratori Nazionali di Frascati, Frascati, Italy

L. Benussi, S. Bianco, F. Fabbri, D. Piccolo, F. Primavera¹⁴

INFN Sezione di Genova ^a, Università di Genova ^b, Genova, Italy

V. Calvelli^{a,b}, F. Ferro^a, M. Lo Vetere^{a,b}, M.R. Monge^{a,b}, E. Robutti^a, S. Tosi^{a,b}

INFN Sezione di Milano-Bicocca ^a, Università di Milano-Bicocca ^b, Milano, Italy

L. Brianza¹⁴, M.E. Dinardo^{a,b}, S. Fiorendi^{a,b}, S. Gennai^a, A. Ghezzi^{a,b}, P. Govoni^{a,b}, S. Malvezzi^a, R.A. Manzoni^{a,b,14}, B. Marzocchi^{a,b}, D. Menasce^a, L. Moroni^a, M. Paganoni^{a,b}, D. Pedrini^a, S. Pigazzini, S. Ragazzi^{a,b}, T. Tabarelli de Fatis^{a,b}

INFN Sezione di Napoli ^a, Università di Napoli 'Federico II' ^b, Napoli, Italy, Università della Basilicata ^c, Potenza, Italy, Università G. Marconi ^d, Roma, Italy

S. Buontempo^a, N. Cavallo^{a,c}, G. De Nardo, S. Di Guida^{a,d,14}, M. Esposito^{a,b}, F. Fabozzi^{a,c}, A.O.M. Iorio^{a,b}, G. Lanza^a, L. Lista^a, S. Meola^{a,d,14}, P. Paolucci^{a,14}, C. Sciacca^{a,b}, F. Thyssen

INFN Sezione di Padova ^a, Università di Padova ^b, Padova, Italy, Università di Trento ^c, Trento, Italy

P. Azzi^{a,14}, N. Bacchetta^a, L. Benato^{a,b}, D. Bisello^{a,b}, A. Boletti^{a,b}, R. Carlin^{a,b}, A. Carvalho Antunes De Oliveira^{a,b}, P. Checchia^a, M. Dall'Osso^{a,b}, P. De Castro Manzano^a, T. Dorigo^a, U. Dosselli^a, F. Gasparini^{a,b}, U. Gasparini^{a,b}, A. Gozzelino^a, S. Lacaprara^a, M. Margoni^{a,b}, A.T. Meneguzzo^{a,b}, J. Pazzini^{a,b,14}, N. Pozzobon^{a,b}, P. Ronchese^{a,b}, F. Simonetto^{a,b}, E. Torassa^a, M. Zanetti, P. Zotto^{a,b}, A. Zucchetta^{a,b}, G. Zumerle^{a,b}

INFN Sezione di Pavia ^a, Università di Pavia ^b, Pavia, Italy

A. Braghieri^a, A. Magnani^{a,b}, P. Montagna^{a,b}, S.P. Ratti^{a,b}, V. Re^a, C. Riccardi^{a,b}, P. Salvini^a, I. Vai^{a,b}, P. Vitulo^{a,b}

INFN Sezione di Perugia ^a, Università di Perugia ^b, Perugia, Italy

L. Alunni Solestizi^{a,b}, G.M. Bilei^a, D. Ciangottini^{a,b}, L. Fanò^{a,b}, P. Lariccia^{a,b}, R. Leonardi^{a,b}, G. Mantovani^{a,b}, M. Menichelli^a, A. Saha^a, A. Santocchia^{a,b}

INFN Sezione di Pisa ^a, Università di Pisa ^b, Scuola Normale Superiore di Pisa ^c, Pisa, Italy

K. Androsov^{a,30}, P. Azzurri^{a,14}, G. Bagliesi^a, J. Bernardini^a, T. Boccali^a, R. Castaldi^a, M.A. Ciocci^{a,30}, R. Dell'Orso^a, S. Donato^{a,c}, G. Fedi, A. Giassi^a, M.T. Grippo^{a,30}, F. Ligabue^{a,c}, T. Lomtadze^a, L. Martini^{a,b}, A. Messineo^{a,b}, F. Palla^a, A. Rizzi^{a,b}, A. Savoy-Navarro^{a,31}, P. Spagnolo^a, R. Tenchini^a, G. Tonelli^{a,b}, A. Venturi^a, P.G. Verdini^a

INFN Sezione di Roma ^a, Università di Roma ^b, Roma, Italy

L. Barone^{a,b}, F. Cavallari^a, M. Cipriani^{a,b}, G. D'imperio^{a,b,14}, D. Del Re^{a,b,14}, M. Diemoz^a, S. Gelli^{a,b}, C. Jorda^a, E. Longo^{a,b}, F. Margaroli^{a,b}, P. Meridiani^a, G. Organtini^{a,b}, R. Paramatti^a, F. Preiato^{a,b}, S. Rahatlou^{a,b}, C. Rovelli^a, F. Santanastasio^{a,b}

INFN Sezione di Torino ^a, Università di Torino ^b, Torino, Italy, Università del Piemonte Orientale ^c, Novara, Italy

N. Amapane^{a,b}, R. Arcidiacono^{a,c,14}, S. Argiro^{a,b}, M. Arneodo^{a,c}, N. Bartosik^a, R. Bellan^{a,b}, C. Biino^a, N. Cartiglia^a, F. Cenna^{a,b}, M. Costa^{a,b}, R. Covarelli^{a,b}, A. Degano^{a,b}, N. Demaria^a, L. Finco^{a,b}, B. Kiani^{a,b}, C. Mariotti^a, S. Maselli^a, E. Migliore^{a,b}, V. Monaco^{a,b}, E. Monteil^{a,b}, M.M. Obertino^{a,b}, L. Pacher^{a,b}, N. Pastrone^a, M. Pelliccioni^a, G.L. Pinna Angioni^{a,b}, F. Ravera^{a,b}

A. Romero^{a,b}, M. Ruspa^{a,c}, R. Sacchi^{a,b}, K. Shchelina^{a,b}, V. Sola^a, A. Solano^{a,b}, A. Staiano^a, P. Traczyk^{a,b}

INFN Sezione di Trieste ^a, Università di Trieste ^b, Trieste, Italy

S. Belforte^a, M. Casarsa^a, F. Cossutti^a, G. Della Ricca^{a,b}, C. La Licata^{a,b}, A. Schizzi^{a,b}, A. Zanetti^a

Kyungpook National University, Daegu, Korea

D.H. Kim, G.N. Kim, M.S. Kim, S. Lee, S.W. Lee, Y.D. Oh, S. Sekmen, D.C. Son, Y.C. Yang

Chonbuk National University, Jeonju, Korea

A. Lee

Hanyang University, Seoul, Korea

J.A. Brochero Cifuentes, T.J. Kim

Korea University, Seoul, Korea

S. Cho, S. Choi, Y. Go, D. Gyun, S. Ha, B. Hong, Y. Jo, Y. Kim, B. Lee, K. Lee, K.S. Lee, S. Lee, J. Lim, S.K. Park, Y. Roh

Seoul National University, Seoul, Korea

J. Almond, J. Kim, S.B. Oh, S.h. Seo, U.K. Yang, H.D. Yoo, G.B. Yu

University of Seoul, Seoul, Korea

M. Choi, H. Kim, H. Kim, J.H. Kim, J.S.H. Lee, I.C. Park, G. Ryu, M.S. Ryu

Sungkyunkwan University, Suwon, Korea

Y. Choi, J. Goh, C. Hwang, J. Lee, I. Yu

Vilnius University, Vilnius, Lithuania

V. Dudenas, A. Juodagalvis, J. Vaitkus

National Centre for Particle Physics, Universiti Malaya, Kuala Lumpur, Malaysia

I. Ahmed, Z.A. Ibrahim, J.R. Komaragiri, M.A.B. Md Ali³², F. Mohamad Idris³³, W.A.T. Wan Abdullah, M.N. Yusli, Z. Zolkapli

Centro de Investigacion y de Estudios Avanzados del IPN, Mexico City, Mexico

H. Castilla-Valdez, E. De La Cruz-Burelo, I. Heredia-De La Cruz³⁴, A. Hernandez-Almada, R. Lopez-Fernandez, R. Magaña Villalba, J. Mejia Guisao, A. Sanchez-Hernandez

Universidad Iberoamericana, Mexico City, Mexico

S. Carrillo Moreno, C. Oropeza Barrera, F. Vazquez Valencia

Benemerita Universidad Autonoma de Puebla, Puebla, Mexico

S. Carpintero, I. Pedraza, H.A. Salazar Ibarguen, C. Uribe Estrada

Universidad Autónoma de San Luis Potosí, San Luis Potosí, Mexico

A. Morelos Pineda

University of Auckland, Auckland, New Zealand

D. Kofcheck

University of Canterbury, Christchurch, New Zealand

P.H. Butler

National Centre for Physics, Quaid-I-Azam University, Islamabad, Pakistan

A. Ahmad, M. Ahmad, Q. Hassan, H.R. Hoorani, W.A. Khan, M.A. Shah, M. Shoaib, M. Waqas

National Centre for Nuclear Research, Swierk, Poland

H. Bialkowska, M. Bluj, B. Boimska, T. Frueboes, M. Górski, M. Kazana, K. Nawrocki, K. Romanowska-Rybinska, M. Szleper, P. Zalewski

Institute of Experimental Physics, Faculty of Physics, University of Warsaw, Warsaw, Poland

K. Bunkowski, A. Byszuk³⁵, K. Doroba, A. Kalinowski, M. Konecki, J. Krolikowski, M. Misiura, M. Olszewski, M. Walczak

Laboratório de Instrumentação e Física Experimental de Partículas, Lisboa, Portugal

P. Bargassa, C. Beirão Da Cruz E Silva, A. Di Francesco, P. Faccioli, P.G. Ferreira Parracho, M. Gallinaro, J. Hollar, N. Leonardo, L. Lloret Iglesias, M.V. Nemallapudi, J. Rodrigues Antunes, J. Seixas, O. Toldaiev, D. Vadruccio, J. Varela, P. Vischia

Joint Institute for Nuclear Research, Dubna, Russia

S. Afanasiev, P. Bunin, I. Golutvin, A. Kamenev, V. Karjavin, V. Korenkov, A. Lanev, A. Malakhov, V. Matveev^{36,37}, V.V. Mitsyn, P. Moisenz, V. Palichik, V. Perelygin, S. Shmatov, N. Skatchkov, V. Smirnov, E. Tikhonenko, B.S. Yuldashev³⁸, A. Zarubin

Petersburg Nuclear Physics Institute, Gatchina (St. Petersburg), Russia

L. Chtchipounov, V. Golovtsov, Y. Ivanov, V. Kim³⁹, E. Kuznetsova⁴⁰, V. Murzin, V. Oreshkin, V. Sulimov, A. Vorobyev

Institute for Nuclear Research, Moscow, Russia

Yu. Andreev, A. Dermenev, S. Gninenko, N. Golubev, A. Karneyeu, M. Kirsanov, N. Krasnikov, A. Pashenkov, D. Tlisov, A. Toropin

Institute for Theoretical and Experimental Physics, Moscow, Russia

V. Epshteyn, V. Gavrilov, N. Lychkovskaya, V. Popov, I. Pozdnyakov, G. Safronov, A. Spiridonov, M. Toms, E. Vlasov, A. Zhokin

Moscow Institute of Physics and Technology

A. Bylinkin³⁷

National Research Nuclear University 'Moscow Engineering Physics Institute' (MEPhI), Moscow, Russia

R. Chistov⁴¹, M. Danilov⁴¹, V. Rusinov

P.N. Lebedev Physical Institute, Moscow, Russia

V. Andreev, M. Azarkin³⁷, I. Dremin³⁷, M. Kirakosyan, A. Leonidov³⁷, S.V. Rusakov, A. Terkulov

Skobeltsyn Institute of Nuclear Physics, Lomonosov Moscow State University, Moscow, Russia

A. Baskakov, A. Belyaev, E. Boos, A. Demiyanov, A. Ershov, A. Gribushin, O. Kodolova, V. Korotkikh, I. Loktin, I. Miagkov, S. Obraztsov, S. Petrushanko, V. Savrin, A. Snigirev, I. Vardanyan

Novosibirsk State University (NSU), Novosibirsk, Russia

V. Blinov⁴², Y. Skovpen⁴²

State Research Center of Russian Federation, Institute for High Energy Physics, Protvino, Russia

I. Azhgirey, I. Bayshev, S. Bitioukov, D. Elumakhov, V. Kachanov, A. Kalinin, D. Konstantinov, V. Krychkine, V. Petrov, R. Ryutin, A. Sobol, S. Troshin, N. Tyurin, A. Uzunian, A. Volkov

University of Belgrade, Faculty of Physics and Vinca Institute of Nuclear Sciences, Belgrade, Serbia

P. Adzic⁴³, P. Cirkovic, D. Devetak, M. Dordevic, J. Milosevic, V. Rekovic

Centro de Investigaciones Energéticas Medioambientales y Tecnológicas (CIEMAT), Madrid, Spain

J. Alcaraz Maestre, M. Barrio Luna, E. Calvo, M. Cerrada, M. Chamizo Llatas, N. Colino, B. De La Cruz, A. Delgado Peris, A. Escalante Del Valle, C. Fernandez Bedoya, J.P. Fernández Ramos, J. Flix, M.C. Fouz, P. Garcia-Abia, O. Gonzalez Lopez, S. Goy Lopez, J.M. Hernandez, M.I. Josa, E. Navarro De Martino, A. Pérez-Calero Yzquierdo, J. Puerta Pelayo, A. Quintario Olmeda, I. Redondo, L. Romero, M.S. Soares

Universidad Autónoma de Madrid, Madrid, Spain

J.F. de Trocóniz, M. Missiroli, D. Moran

Universidad de Oviedo, Oviedo, Spain

J. Cuevas, J. Fernandez Menendez, I. Gonzalez Caballero, J.R. González Fernández, E. Palencia Cortezon, S. Sanchez Cruz, I. Suárez Andrés, J.M. Vizan Garcia

Instituto de Física de Cantabria (IFCA), CSIC-Universidad de Cantabria, Santander, Spain

I.J. Cabrillo, A. Calderon, J.R. Castiñeiras De Saa, E. Curras, M. Fernandez, J. Garcia-Ferrero, G. Gomez, A. Lopez Virto, J. Marco, C. Martinez Rivero, F. Matorras, J. Piedra Gomez, T. Rodrigo, A. Ruiz-Jimeno, L. Scodellaro, N. Trevisani, I. Vila, R. Vilar Cortabitarte

CERN, European Organization for Nuclear Research, Geneva, Switzerland

D. Abbaneo, E. Auffray, G. Auzinger, M. Bachtis, P. Baillon, A.H. Ball, D. Barney, P. Bloch, A. Bocci, A. Bonato, C. Botta, T. Camporesi, R. Castello, M. Cepeda, G. Cerminara, M. D'Alfonso, D. d'Enterria, A. Dabrowski, V. Daponte, A. David, M. De Gruttola, F. De Guio, A. De Roeck, E. Di Marco⁴⁴, M. Dobson, B. Dorney, T. du Pree, D. Duggan, M. Dünser, N. Dupont, A. Elliott-Peisert, S. Fartoukh, G. Franzoni, J. Fulcher, W. Funk, D. Gigi, K. Gill, M. Girone, F. Glege, D. Gulhan, S. Gundacker, M. Guthoff, J. Hammer, P. Harris, J. Hegeman, V. Innocente, P. Janot, H. Kirschenmann, V. Knünz, A. Kornmayer¹⁴, M.J. Kortelainen, K. Kousouris, M. Krammer¹, P. Lecoq, C. Lourenço, M.T. Lucchini, L. Malgeri, M. Mannelli, A. Martelli, F. Meijers, S. Mersi, E. Meschi, F. Moortgat, S. Morovic, M. Mulders, H. Neugebauer, S. Orfanelli, L. Orsini, L. Pape, E. Perez, M. Peruzzi, A. Petrilli, G. Petrucciani, A. Pfeiffer, M. Pierini, A. Racz, T. Reis, G. Rolandi⁴⁵, M. Rovere, M. Ruan, H. Sakulin, J.B. Sauvan, C. Schäfer, C. Schwick, M. Seidel, A. Sharma, P. Silva, M. Simon, P. Sphicas⁴⁶, J. Steggemann, M. Stoye, Y. Takahashi, M. Tosi, D. Treille, A. Triossi, A. Tsirou, V. Veckalns⁴⁷, G.I. Veres²¹, N. Wardle, A. Zagozdzinska³⁵, W.D. Zeuner

Paul Scherrer Institut, Villigen, Switzerland

W. Bertl, K. Deiters, W. Erdmann, R. Horisberger, Q. Ingram, H.C. Kaestli, D. Kotlinski, U. Langenegger, T. Rohe

Institute for Particle Physics, ETH Zurich, Zurich, Switzerland

F. Bachmair, L. Bäni, L. Bianchini, B. Casal, G. Dissertori, M. Dittmar, M. Donegà, P. Eller, C. Grab, C. Heidegger, D. Hits, J. Hoss, G. Kasieczka, P. Lecomte[†], W. Lustermann, B. Mangano, M. Marionneau, P. Martinez Ruiz del Arbol, M. Masciovecchio, M.T. Meinhard, D. Meister, F. Micheli, P. Musella, F. Nessi-Tedaldi, F. Pandolfi, J. Pata, F. Pauss, G. Perrin, L. Perrozzi, M. Quitnat, M. Rossini, M. Schönenberger, A. Starodumov⁴⁸, V.R. Tavolaro, K. Theofilatos, R. Wallny

Universität Zürich, Zurich, Switzerland

T.K. Aarrestad, C. Amsler⁴⁹, L. Caminada, M.F. Canelli, A. De Cosa, C. Galloni, A. Hinzmann, T. Hreus, B. Kilminster, C. Lange, J. Ngadiuba, D. Pinna, G. Rauco, P. Robmann, D. Salerno, Y. Yang

National Central University, Chung-Li, Taiwan

V. Candelise, T.H. Doan, Sh. Jain, R. Khurana, M. Konyushikhin, C.M. Kuo, W. Lin, Y.J. Lu, A. Pozdnyakov, S.S. Yu

National Taiwan University (NTU), Taipei, Taiwan

Arun Kumar, P. Chang, Y.H. Chang, Y.W. Chang, Y. Chao, K.F. Chen, P.H. Chen, C. Dietz, F. Fiori, W.-S. Hou, Y. Hsiung, Y.F. Liu, R.-S. Lu, M. Miñano Moya, E. Paganis, A. Psallidas, J.f. Tsai, Y.M. Tzeng

Chulalongkorn University, Faculty of Science, Department of Physics, Bangkok, Thailand

B. Asavapibhop, G. Singh, N. Srimanobhas, N. Suwonjandee

Cukurova University, Adana, Turkey

A. Adiguzel, S. Cerci⁵⁰, S. Damarseckin, Z.S. Demiroglu, C. Dozen, I. Dumanoglu, S. Girgis, G. Gokbulut, Y. Guler, E. Gurpinar, I. Hos, E.E. Kangal⁵¹, O. Kara, A. Kayis Topaksu, U. Kiminsu, M. Oglakci, G. Onengut⁵², K. Ozdemir⁵³, D. Sunar Cerci⁵⁰, H. Topakli⁵⁴, S. Turkcapar, I.S. Zorbakir, C. Zorbilmez

Middle East Technical University, Physics Department, Ankara, Turkey

B. Bilin, S. Bilmis, B. Isildak⁵⁵, G. Karapinar⁵⁶, M. Yalvac, M. Zeyrek

Bogazici University, Istanbul, Turkey

E. Gürmez, M. Kaya⁵⁷, O. Kaya⁵⁸, E.A. Yetkin⁵⁹, T. Yetkin⁶⁰

Istanbul Technical University, Istanbul, Turkey

A. Cakir, K. Cankocak, S. Sen⁶¹

Institute for Scintillation Materials of National Academy of Science of Ukraine, Kharkov, Ukraine

B. Grynyov

National Scientific Center, Kharkov Institute of Physics and Technology, Kharkov, Ukraine

L. Levchuk, P. Sorokin

University of Bristol, Bristol, United Kingdom

R. Aggleton, F. Ball, L. Beck, J.J. Brooke, D. Burns, E. Clement, D. Cussans, H. Flacher, J. Goldstein, M. Grimes, G.P. Heath, H.F. Heath, J. Jacob, L. Kreczko, C. Lucas, D.M. Newbold⁶², S. Paramesvaran, A. Poll, T. Sakuma, S. Seif El Nasr-storey, D. Smith, V.J. Smith

Rutherford Appleton Laboratory, Didcot, United Kingdom

D. Barducci, A. Belyaev⁶³, C. Brew, R.M. Brown, L. Calligaris, D. Cieri, D.J.A. Cockerill, J.A. Coughlan, K. Harder, S. Harper, E. Olaiya, D. Petyt, C.H. Shepherd-Themistocleous, A. Thea, I.R. Tomalin, T. Williams

Imperial College, London, United Kingdom

M. Baber, R. Bainbridge, O. Buchmuller, A. Bundock, D. Burton, S. Casasso, M. Citron, D. Colling, L. Corpe, P. Dauncey, G. Davies, A. De Wit, M. Della Negra, R. Di Maria, P. Dunne, A. Elwood, D. Futyan, Y. Haddad, G. Hall, G. Iles, T. James, R. Lane, C. Laner, R. Lucas⁶², L. Lyons, A.-M. Magnan, S. Malik, L. Mastrolorenzo, J. Nash, A. Nikitenko⁴⁸, J. Pela, B. Penning,

M. Pesaresi, D.M. Raymond, A. Richards, A. Rose, C. Seez, S. Summers, A. Tapper, K. Uchida, M. Vazquez Acosta⁶⁴, T. Virdee¹⁴, J. Wright, S.C. Zenz

Brunel University, Uxbridge, United Kingdom

J.E. Cole, P.R. Hobson, A. Khan, P. Kyberd, D. Leslie, I.D. Reid, P. Symonds, L. Teodorescu, M. Turner

Baylor University, Waco, USA

A. Borzou, K. Call, J. Dittmann, K. Hatakeyama, H. Liu, N. Pastika

The University of Alabama, Tuscaloosa, USA

O. Charaf, S.I. Cooper, C. Henderson, P. Rumerio

Boston University, Boston, USA

D. Arcaro, A. Avetisyan, T. Bose, D. Gastler, D. Rankin, C. Richardson, J. Rohlf, L. Sulak, D. Zou

Brown University, Providence, USA

G. Benelli, E. Berry, D. Cutts, A. Garabedian, J. Hakala, U. Heintz, J.M. Hogan, O. Jesus, E. Laird, G. Landsberg, Z. Mao, M. Narain, S. Piperov, S. Sagir, E. Spencer, R. Syarif

University of California, Davis, USA

R. Breedon, G. Breto, D. Burns, M. Calderon De La Barca Sanchez, S. Chauhan, M. Chertok, J. Conway, R. Conway, P.T. Cox, R. Erbacher, C. Flores, G. Funk, M. Gardner, W. Ko, R. Lander, C. Mclean, M. Mulhearn, D. Pellett, J. Pilot, F. Ricci-Tam, S. Shalhout, J. Smith, M. Squires, D. Stolp, M. Tripathi, S. Wilbur, R. Yohay

University of California, Los Angeles, USA

R. Cousins, P. Everaerts, A. Florent, J. Hauser, M. Ignatenko, D. Saltzberg, E. Takasugi, V. Valuev, M. Weber

University of California, Riverside, Riverside, USA

K. Burt, R. Clare, J. Ellison, J.W. Gary, G. Hanson, J. Heilman, P. Jandir, E. Kennedy, F. Lacroix, O.R. Long, M. Malberti, M. Olmedo Negrete, M.I. Paneva, A. Shrinivas, H. Wei, S. Wimpenny, B. R. Yates

University of California, San Diego, La Jolla, USA

J.G. Branson, G.B. Cerati, S. Cittolin, M. Derdzinski, R. Gerosa, A. Holzner, D. Klein, V. Krutelyov, J. Letts, I. Macneill, D. Olivito, S. Padhi, M. Pieri, M. Sani, V. Sharma, S. Simon, M. Tadel, A. Vartak, S. Wasserbaech⁶⁵, C. Welke, J. Wood, F. Würthwein, A. Yagil, G. Zevi Della Porta

University of California, Santa Barbara - Department of Physics, Santa Barbara, USA

R. Bhandari, J. Bradmiller-Feld, C. Campagnari, A. Dishaw, V. Dutta, K. Flowers, M. Franco Sevilla, P. Geffert, C. George, F. Golf, L. Gouskos, J. Gran, R. Heller, J. Incandela, N. Mccoll, S.D. Mullin, A. Ovcharova, J. Richman, D. Stuart, I. Suarez, C. West, J. Yoo

California Institute of Technology, Pasadena, USA

D. Anderson, A. Apresyan, J. Bendavid, A. Bornheim, J. Bunn, Y. Chen, J. Duarte, J.M. Lawhorn, A. Mott, H.B. Newman, C. Pena, M. Spiropulu, J.R. Vlimant, S. Xie, R.Y. Zhu

Carnegie Mellon University, Pittsburgh, USA

M.B. Andrews, V. Azzolini, T. Ferguson, M. Paulini, J. Russ, M. Sun, H. Vogel, I. Vorobiev

University of Colorado Boulder, Boulder, USA

J.P. Cumalat, W.T. Ford, F. Jensen, A. Johnson, M. Krohn, T. Mulholland, K. Stenson, S.R. Wagner

Cornell University, Ithaca, USA

J. Alexander, J. Chaves, J. Chu, S. Dittmer, K. Mcdermott, N. Mirman, G. Nicolas Kaufman, J.R. Patterson, A. Rinkevicius, A. Ryd, L. Skinnari, L. Soffi, S.M. Tan, Z. Tao, J. Thom, J. Tucker, P. Wittich, M. Zientek

Fairfield University, Fairfield, USA

D. Winn

Fermi National Accelerator Laboratory, Batavia, USA

S. Abdullin, M. Albrow, G. Apollinari, S. Banerjee, L.A.T. Bauerick, A. Beretvas, J. Berryhill, P.C. Bhat, G. Bolla, K. Burkett, J.N. Butler, H.W.K. Cheung, F. Chlebana, S. Cihangir[†], M. Cremonesi, V.D. Elvira, I. Fisk, J. Freeman, E. Gottschalk, L. Gray, D. Green, S. Grünendahl, O. Gutsche, D. Hare, R.M. Harris, S. Hasegawa, J. Hirschauer, Z. Hu, B. Jayatilaka, S. Jindariani, M. Johnson, U. Joshi, B. Klima, B. Kreis, S. Lammel, J. Linacre, D. Lincoln, R. Lipton, T. Liu, R. Lopes De Sá, J. Lykken, K. Maeshima, N. Magini, J.M. Marraffino, S. Maruyama, D. Mason, P. McBride, P. Merkel, S. Mrenna, S. Nahm, C. Newman-Holmes[†], V. O'Dell, K. Pedro, O. Prokofyev, G. Rakness, L. Ristori, E. Sexton-Kennedy, A. Soha, W.J. Spalding, L. Spiegel, S. Stoynev, N. Strobbe, L. Taylor, S. Tkaczyk, N.V. Tran, L. Uplegger, E.W. Vaandering, C. Vernieri, M. Verzocchi, R. Vidal, M. Wang, H.A. Weber, A. Whitbeck

University of Florida, Gainesville, USA

D. Acosta, P. Avery, P. Bortignon, D. Bourilkov, A. Brinkerhoff, A. Carnes, M. Carver, D. Curry, S. Das, R.D. Field, I.K. Furic, J. Konigsberg, A. Korytov, P. Ma, K. Matchev, H. Mei, P. Milenovic⁶⁶, G. Mitselmakher, D. Rank, L. Shchutska, D. Sperka, L. Thomas, J. Wang, S. Wang, J. Yelton

Florida International University, Miami, USA

S. Linn, P. Markowitz, G. Martinez, J.L. Rodriguez

Florida State University, Tallahassee, USA

A. Ackert, J.R. Adams, T. Adams, A. Askew, S. Bein, B. Diamond, S. Hagopian, V. Hagopian, K.F. Johnson, A. Khatiwada, H. Prosper, A. Santra, M. Weinberg

Florida Institute of Technology, Melbourne, USA

M.M. Baarmand, V. Bhopatkar, S. Colafranceschi⁶⁷, M. Hohlmann, D. Noonan, T. Roy, F. Yumiceva

University of Illinois at Chicago (UIC), Chicago, USA

M.R. Adams, L. Apanasevich, D. Berry, R.R. Betts, I. Bucinskaite, R. Cavanaugh, O. Evdokimov, L. Gauthier, C.E. Gerber, D.J. Hofman, P. Kurt, C. O'Brien, I.D. Sandoval Gonzalez, H. Trauger, P. Turner, N. Varelas, H. Wang, Z. Wu, M. Zakaria, J. Zhang

The University of Iowa, Iowa City, USA

B. Bilki⁶⁸, W. Clarida, K. Dilsiz, S. Durgut, R.P. Gundrajula, M. Haytmyradov, V. Khristenko, J.-P. Merlo, H. Mermerkaya⁶⁹, A. Mestvirishvili, A. Moeller, J. Nachtman, H. Ogul, Y. Onel, F. Ozok⁷⁰, A. Penzo, C. Snyder, E. Tiras, J. Wetzel, K. Yi

Johns Hopkins University, Baltimore, USA

I. Anderson, B. Blumenfeld, A. Cocoros, N. Eminizer, D. Fehling, L. Feng, A.V. Gritsan, P. Maksimovic, M. Osherson, J. Roskes, U. Sarica, M. Swartz, M. Xiao, Y. Xin, C. You

The University of Kansas, Lawrence, USA

A. Al-bataineh, P. Baringer, A. Bean, J. Bowen, C. Bruner, J. Castle, R.P. Kenny III,

A. Kropivnitskaya, D. Majumder, W. Mcbrayer, M. Murray, S. Sanders, R. Stringer, J.D. Tapia Takaki, Q. Wang

Kansas State University, Manhattan, USA

A. Ivanov, K. Kaadze, S. Khalil, M. Makouski, Y. Maravin, A. Mohammadi, L.K. Saini, N. Skhirtladze, S. Toda

Lawrence Livermore National Laboratory, Livermore, USA

F. Rebassoo, D. Wright

University of Maryland, College Park, USA

C. Anelli, A. Baden, O. Baron, A. Belloni, B. Calvert, S.C. Eno, C. Ferraioli, J.A. Gomez, N.J. Hadley, S. Jabeen, R.G. Kellogg, T. Kolberg, J. Kunkle, Y. Lu, A.C. Mignerey, Y.H. Shin, A. Skuja, M.B. Tonjes, S.C. Tonwar

Massachusetts Institute of Technology, Cambridge, USA

D. Abercrombie, B. Allen, A. Apyan, R. Barbieri, A. Baty, R. Bi, K. Bierwagen, S. Brandt, W. Busza, I.A. Cali, Z. Demiragli, L. Di Matteo, G. Gomez Ceballos, M. Goncharov, D. Hsu, Y. Iiyama, G.M. Innocenti, M. Klute, D. Kovalevskyi, K. Krafczak, Y.S. Lai, Y.-J. Lee, A. Levin, P.D. Luckey, A.C. Marini, C. McGinn, C. Mironov, S. Narayanan, X. Niu, C. Paus, C. Roland, G. Roland, J. Salfeld-Nebgen, G.S.F. Stephans, K. Sumorok, K. Tatar, M. Varma, D. Velicanu, J. Veverka, J. Wang, T.W. Wang, B. Wyslouch, M. Yang, V. Zhukova

University of Minnesota, Minneapolis, USA

A.C. Benvenuti, R.M. Chatterjee, A. Evans, A. Finkel, A. Gude, P. Hansen, S. Kalafut, S.C. Kao, Y. Kubota, Z. Lesko, J. Mans, S. Nourbakhsh, N. Ruckstuhl, R. Rusack, N. Tambe, J. Turkewitz

University of Mississippi, Oxford, USA

J.G. Acosta, S. Oliveros

University of Nebraska-Lincoln, Lincoln, USA

E. Avdeeva, R. Bartek, K. Bloom, D.R. Claes, A. Dominguez, C. Fangmeier, R. Gonzalez Suarez, R. Kamalieddin, I. Kravchenko, A. Malta Rodrigues, F. Meier, J. Monroy, J.E. Siado, G.R. Snow, B. Stieger

State University of New York at Buffalo, Buffalo, USA

M. Alyari, J. Dolen, J. George, A. Godshalk, C. Harrington, I. Iashvili, J. Kaisen, A. Kharchilava, A. Kumar, A. Parker, S. Rappoccio, B. Roozbahani

Northeastern University, Boston, USA

G. Alverson, E. Barberis, D. Baumgartel, A. Hortiangtham, B. Knapp, A. Massironi, D.M. Morse, D. Nash, T. Orimoto, R. Teixeira De Lima, D. Trocino, R.-J. Wang, D. Wood

Northwestern University, Evanston, USA

S. Bhattacharya, K.A. Hahn, A. Kubik, A. Kumar, J.F. Low, N. Mucia, N. Odell, B. Pollack, M.H. Schmitt, K. Sung, M. Trovato, M. Velasco

University of Notre Dame, Notre Dame, USA

N. Dev, M. Hildreth, K. Hurtado Anampa, C. Jessop, D.J. Karmgard, N. Kellams, K. Lannon, N. Marinelli, F. Meng, C. Mueller, Y. Musienko³⁶, M. Planer, A. Reinsvold, R. Ruchti, G. Smith, S. Taroni, N. Valls, M. Wayne, M. Wolf, A. Woodard

The Ohio State University, Columbus, USA

J. Alimena, L. Antonelli, J. Brinson, B. Bylsma, L.S. Durkin, S. Flowers, B. Francis, A. Hart, C. Hill, R. Hughes, W. Ji, B. Liu, W. Luo, D. Puigh, B.L. Winer, H.W. Wulsin

Princeton University, Princeton, USA

S. Cooperstein, O. Driga, P. Elmer, J. Hardenbrook, P. Hebda, D. Lange, J. Luo, D. Marlow, T. Medvedeva, K. Mei, M. Mooney, J. Olsen, C. Palmer, P. Piroué, D. Stickland, C. Tully, A. Zuranski

University of Puerto Rico, Mayaguez, USA

S. Malik

Purdue University, West Lafayette, USA

A. Barker, V.E. Barnes, S. Folgueras, L. Gutay, M.K. Jha, M. Jones, A.W. Jung, K. Jung, D.H. Miller, N. Neumeister, B.C. Radburn-Smith, X. Shi, J. Sun, A. Svyatkovskiy, F. Wang, W. Xie, L. Xu

Purdue University Calumet, Hammond, USA

N. Parashar, J. Stupak

Rice University, Houston, USA

A. Adair, B. Akgun, Z. Chen, K.M. Ecklund, F.J.M. Geurts, M. Guilbaud, W. Li, B. Michlin, M. Northup, B.P. Padley, R. Redjimi, J. Roberts, J. Rorie, Z. Tu, J. Zabel

University of Rochester, Rochester, USA

B. Betchart, A. Bodek, P. de Barbaro, R. Demina, Y.t. Duh, T. Ferbel, M. Galanti, A. Garcia-Bellido, J. Han, O. Hindrichs, A. Khukhunaishvili, K.H. Lo, P. Tan, M. Verzetti

Rutgers, The State University of New Jersey, Piscataway, USA

J.P. Chou, E. Contreras-Campana, Y. Gershtein, T.A. Gómez Espinosa, E. Halkiadakis, M. Heindl, D. Hidas, E. Hughes, S. Kaplan, R. Kunnnawalkam Elayavalli, S. Kyriacou, A. Lath, K. Nash, H. Saka, S. Salur, S. Schnetzer, D. Sheffield, S. Somalwar, R. Stone, S. Thomas, P. Thomassen, M. Walker

University of Tennessee, Knoxville, USA

M. Foerster, J. Heideman, G. Riley, K. Rose, S. Spanier, K. Thapa

Texas A&M University, College Station, USA

O. Bouhali⁷¹, A. Celik, M. Dalchenko, M. De Mattia, A. Delgado, S. Dildick, R. Eusebi, J. Gilmore, T. Huang, E. Juska, T. Kamon⁷², R. Mueller, Y. Pakhotin, R. Patel, A. Perloff, L. Perniè, D. Rathjens, A. Rose, A. Safonov, A. Tatarinov, K.A. Ulmer

Texas Tech University, Lubbock, USA

N. Akchurin, C. Cowden, J. Damgov, C. Dragoiu, P.R. Dudero, J. Faulkner, S. Kunori, K. Lamichhane, S.W. Lee, T. Libeiro, S. Undleeb, I. Volobouev, Z. Wang

Vanderbilt University, Nashville, USA

A.G. Delannoy, S. Greene, A. Gurrola, R. Janjam, W. Johns, C. Maguire, A. Melo, H. Ni, P. Sheldon, S. Tuo, J. Velkovska, Q. Xu

University of Virginia, Charlottesville, USA

M.W. Areenton, P. Barria, B. Cox, J. Goodell, R. Hirosky, A. Ledovskoy, H. Li, C. Neu, T. Sinthuprasith, X. Sun, Y. Wang, E. Wolfe, F. Xia

Wayne State University, Detroit, USA

C. Clarke, R. Harr, P.E. Karchin, P. Lamichhane, J. Sturdy

University of Wisconsin - Madison, Madison, WI, USA

D.A. Belknap, S. Dasu, L. Dodd, S. Duric, B. Gomber, M. Grothe, M. Herndon, A. Hervé,

P. Klabbers, A. Lanaro, A. Levine, K. Long, R. Loveless, I. Ojalvo, T. Perry, G.A. Pierro, G. Polese, T. Ruggles, A. Savin, A. Sharma, N. Smith, W.H. Smith, D. Taylor, N. Woods

†: Deceased

- 1: Also at Vienna University of Technology, Vienna, Austria
- 2: Also at State Key Laboratory of Nuclear Physics and Technology, Peking University, Beijing, China
- 3: Also at Institut Pluridisciplinaire Hubert Curien, Université de Strasbourg, Université de Haute Alsace Mulhouse, CNRS/IN2P3, Strasbourg, France
- 4: Also at Universidade Estadual de Campinas, Campinas, Brazil
- 5: Also at Universidade Federal de Pelotas, Pelotas, Brazil
- 6: Also at Université Libre de Bruxelles, Bruxelles, Belgium
- 7: Also at Deutsches Elektronen-Synchrotron, Hamburg, Germany
- 8: Also at Joint Institute for Nuclear Research, Dubna, Russia
- 9: Also at Cairo University, Cairo, Egypt
- 10: Also at Fayoum University, El-Fayoum, Egypt
- 11: Now at British University in Egypt, Cairo, Egypt
- 12: Now at Ain Shams University, Cairo, Egypt
- 13: Also at Université de Haute Alsace, Mulhouse, France
- 14: Also at CERN, European Organization for Nuclear Research, Geneva, Switzerland
- 15: Also at Skobeltsyn Institute of Nuclear Physics, Lomonosov Moscow State University, Moscow, Russia
- 16: Also at Tbilisi State University, Tbilisi, Georgia
- 17: Also at RWTH Aachen University, III. Physikalisches Institut A, Aachen, Germany
- 18: Also at University of Hamburg, Hamburg, Germany
- 19: Also at Brandenburg University of Technology, Cottbus, Germany
- 20: Also at Institute of Nuclear Research ATOMKI, Debrecen, Hungary
- 21: Also at MTA-ELTE Lendület CMS Particle and Nuclear Physics Group, Eötvös Loránd University, Budapest, Hungary
- 22: Also at University of Debrecen, Debrecen, Hungary
- 23: Also at Indian Institute of Science Education and Research, Bhopal, India
- 24: Also at Institute of Physics, Bhubaneswar, India
- 25: Also at University of Visva-Bharati, Santiniketan, India
- 26: Also at University of Ruhuna, Matara, Sri Lanka
- 27: Also at Isfahan University of Technology, Isfahan, Iran
- 28: Also at University of Tehran, Department of Engineering Science, Tehran, Iran
- 29: Also at Plasma Physics Research Center, Science and Research Branch, Islamic Azad University, Tehran, Iran
- 30: Also at Università degli Studi di Siena, Siena, Italy
- 31: Also at Purdue University, West Lafayette, USA
- 32: Also at International Islamic University of Malaysia, Kuala Lumpur, Malaysia
- 33: Also at Malaysian Nuclear Agency, MOSTI, Kajang, Malaysia
- 34: Also at Consejo Nacional de Ciencia y Tecnología, Mexico city, Mexico
- 35: Also at Warsaw University of Technology, Institute of Electronic Systems, Warsaw, Poland
- 36: Also at Institute for Nuclear Research, Moscow, Russia
- 37: Now at National Research Nuclear University 'Moscow Engineering Physics Institute' (MEPhI), Moscow, Russia
- 38: Also at Institute of Nuclear Physics of the Uzbekistan Academy of Sciences, Tashkent, Uzbekistan
- 39: Also at St. Petersburg State Polytechnical University, St. Petersburg, Russia

- 40: Also at University of Florida, Gainesville, USA
41: Also at P.N. Lebedev Physical Institute, Moscow, Russia
42: Also at Budker Institute of Nuclear Physics, Novosibirsk, Russia
43: Also at Faculty of Physics, University of Belgrade, Belgrade, Serbia
44: Also at INFN Sezione di Roma; Università di Roma, Roma, Italy
45: Also at Scuola Normale e Sezione dell'INFN, Pisa, Italy
46: Also at National and Kapodistrian University of Athens, Athens, Greece
47: Also at Riga Technical University, Riga, Latvia
48: Also at Institute for Theoretical and Experimental Physics, Moscow, Russia
49: Also at Albert Einstein Center for Fundamental Physics, Bern, Switzerland
50: Also at Adiyaman University, Adiyaman, Turkey
51: Also at Mersin University, Mersin, Turkey
52: Also at Cag University, Mersin, Turkey
53: Also at Piri Reis University, Istanbul, Turkey
54: Also at Gaziosmanpasa University, Tokat, Turkey
55: Also at Ozyegin University, Istanbul, Turkey
56: Also at Izmir Institute of Technology, Izmir, Turkey
57: Also at Marmara University, Istanbul, Turkey
58: Also at Kafkas University, Kars, Turkey
59: Also at Istanbul Bilgi University, Istanbul, Turkey
60: Also at Yildiz Technical University, Istanbul, Turkey
61: Also at Hacettepe University, Ankara, Turkey
62: Also at Rutherford Appleton Laboratory, Didcot, United Kingdom
63: Also at School of Physics and Astronomy, University of Southampton, Southampton, United Kingdom
64: Also at Instituto de Astrofísica de Canarias, La Laguna, Spain
65: Also at Utah Valley University, Orem, USA
66: Also at University of Belgrade, Faculty of Physics and Vinca Institute of Nuclear Sciences, Belgrade, Serbia
67: Also at Facoltà Ingegneria, Università di Roma, Roma, Italy
68: Also at Argonne National Laboratory, Argonne, USA
69: Also at Erzincan University, Erzincan, Turkey
70: Also at Mimar Sinan University, Istanbul, Istanbul, Turkey
71: Also at Texas A&M University at Qatar, Doha, Qatar
72: Also at Kyungpook National University, Daegu, Korea